

# Highly excited atomic states

B. M. Smirnov

*I. V. Kurchatov Institute of Atomic Energy*  
Usp. Fiz. Nauk **131**, 577–616 (August 1980)

The properties of highly excited atoms are examined. Methods for producing and detecting such atoms are analyzed. Various processes that involve atoms in Rydberg states are described, including transitions between high-lying excited states induced by collisions with electrons and atoms, quenching by electrons and atoms, ionization by collisions with electrons, atoms, and molecules, charge exchange with ions, and so on.

PACS numbers: 31.50. + w, 34.50.Hc, 34.70. + e, 34.80.Dp

## CONTENTS

1. Introduction .....	450
2. Production of atoms in Rydberg states .....	451
3. Radiative transitions of highly excited atoms .....	454
4. Methods for detecting atoms in Rydberg states .....	457
5. Collisions between highly excited atoms and charged particles .....	459
6. Ionization of a highly excited atom as a result of a collision with atomic particles .....	463
7. Quenching of atomic Rydberg states by collisions with atoms and molecules .....	465
8. Conclusions .....	468
References .....	468

## 1. INTRODUCTION

Highly excited atomic states are referred to as Rydberg states. Atoms in such states are very large; their dimensions are of the order of  $a_0 n^2$ , where  $a_0$  is the Bohr radius and  $n$  is the principal quantum number. An excited electron in a Rydberg atom moves in the Coulomb field of the atomic core. The study of the level structure of atomic Rydberg states provides information concerning various types of interactions in the atom, which determine deviations from Coulomb law describing the interaction of the electron with the atomic core and, which, for this reason, appear as perturbations.

Atoms in Rydberg states are of interest to astrophysics. Transitions between the Rydberg states of the hydrogen atom are responsible for the recombination lines in the radio emission spectrum.<sup>1-7</sup> The observation of these lines gives information about interstellar hydrogen. In the mid-1960's, a great deal of attention was directed toward hydrogen atoms in Rydberg states in connection with the possibility of injecting excited hydrogen atoms with  $n=9-15$  into a hot plasma and using this technique for producing a plasma for thermonuclear fusion.<sup>8-10</sup> Subsequent studies demonstrated that this method could not compete with other methods for producing a plasma.

The great interest in atomic Rydberg states in recent years is related to the development of new methods for producing highly excited atoms with the use of a tunable laser. These methods permit excitation of atoms into selected levels and investigation of various processes that involve highly excited atoms in selected states. Such studies provide qualitatively new information concerning processes involving highly excited

atoms. This is the reason for writing the present review.

The creation of experimental techniques that allow production of atoms in a selected highly excited state is also important for applications. Masers have been constructed using transitions between highly excited states.<sup>11,12</sup> Atomic Rydberg states are used for detecting long wavelength radiation,<sup>13-15,167,168</sup> in particular, thermal radiation emitted by solids with surface temperatures below room temperature.

As long as we consider only the Coulomb interactions between an electron and the atomic core, the electron energy of a highly excited atom is given in atomic units<sup>1)</sup> by<sup>16,17</sup>

$$\varepsilon = -\frac{1}{2n^2}, \quad (1)$$

where  $n$  is the principal quantum number of the state. The state is  $2n^2$ -fold degenerate (two-fold degenerate with respect to the electron spin and  $n^2$ -fold degenerate with respect to the spatial quantum numbers). This degeneracy is partially removed by taking into account the non-Coulomb interactions of the electron with the atomic core. Denoting the operator for the non-Coulomb interactions by  $V$ , we find that the shift in the level with principal quantum number  $n$  as a result of this interaction is given by

$$\Delta\varepsilon = \langle \psi_n | V | \psi_n \rangle, \quad (2)$$

where  $\psi_n$  is the wave function of the highly excited electron. Since the interaction  $V$  is appreciable in a region of the order of the dimensions of the atomic core, where

<sup>1)</sup> Here and subsequently we will use atomic units  $\hbar = m_e = e^2 = 1$ .

TABLE I. Quantum defect for the helium atom.<sup>18,19</sup>

State	<sup>3</sup> S	<sup>1</sup> S	<sup>3</sup> P	<sup>1</sup> P	D	F	G
Quantum defect	0.30	0.14	0.07	0.01	0.003	3·10 <sup>-4</sup>	5·10 <sup>-4</sup>

$\psi_n \sim n^{-3/2}$ , we have

$$\Delta\varepsilon = \frac{A}{n^3}. \quad (3)$$

We will assume that the non-Coulomb interactions of the electron with the atomic core are spherically symmetrical. Then this interaction partially removes the Coulomb degeneracy and the states of the highly excited atom are characterized by the quantum numbers  $nlm$  ( $l$  denotes the orbital angular momentum and  $m$  its projection). We will represent the shift in the level as a result of the non-Coulomb interactions in the form  $\Delta\varepsilon_{nl} = -\delta_l/n^3$ , where  $\delta_l$  is the so-called quantum defect, which depends only on the orbital angular momentum of the state. Adding this increment to the electron energy (1), we represent the electron energy of the highly excited atom in the form

$$\varepsilon_{nl} = -\frac{1}{2(n-\delta_l)^2}. \quad (4)$$

From general considerations, it follows that the quantum defect decreases sharply with increasing orbital angular momentum because the probability of finding the highly excited electron in the region occupied by the atomic core drops sharply in this case. This fact is demonstrated in Table I, which displays the quantum defect for a highly excited helium atom. It is evident that the quantum defect drops sharply with increasing orbital angular momentum and formulas (1) and (4) give approximately equal results. Table II shows the interactions that contribute to the quantum defect. The quantum defect is mainly determined by the electrostatic interaction of the excited electron with the atomic core when the highly excited electron penetrates into the atomic core.

Equation (4) can be written in the form

$$\varepsilon_{nl} = -\frac{1}{2(n^*)^2}, \quad (4a)$$

which introduces the effective principal quantum number  $n^*$ . This method of representing the binding energy

TABLE II. Contribution of various interaction mechanisms to the quantum defect for the D-state of the helium atom.<sup>19</sup>

Interaction	Contribution to quantum defect, 10 <sup>-4</sup>
1. Polarization of the atomic core by the outer electron	24
2. Electron exchange interaction	7
3. Screening of the inner electron by the outer electron	2
4. Spin-spin and spin-orbit interactions	1
5. Other interactions	0.2
Sum	34

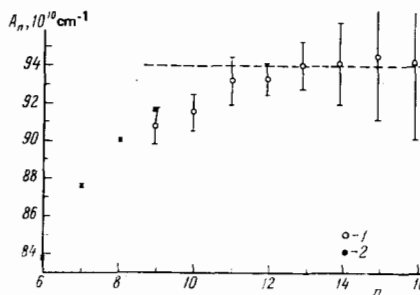


FIG. 1. Fine-structure splitting of the  $D_{3/2}-D_{5/2}$  states of the sodium atom. Experiment: 1—Ref. 20; 2—Ref. 21; dashed line corresponds to the asymptotic limit for  $n \rightarrow \infty$ .

of the electron is mainly applicable to heavy atoms, for which the difference  $\delta_l = n - n^*$  can attain several units (see Ref. 11). Indeed, the principal quantum number is enumerated beginning with the inner electrons of the atom, so that the valence electron in an unexcited heavy atom is characterized by a principal quantum that equals several units, while its ionization potential corresponds to  $n^* = 1-2$ . For example, for a rubidium atom (the outer electron shell of the atom in the ground state is  $5s$ ), the quantity  $\delta_l = n - n^*$  equals<sup>11, 54</sup> 3.16 for  $^2S$  states, 2.69 for  $^2P$  states, and 1.40 for  $^2D$  states. For a strontium atom (the outer electron shell of the atom in the ground state is  $5s^2$ ), the quantity  $\delta_l = n - n^*$  equals<sup>11, 17</sup> 3.27 for highly excited  $^1S$  states, 2.73 for  $^1P$  states, and 2.37 for  $^1, ^3D$  states.<sup>2)</sup>

We note that the dependence on the principal quantum number shown in Eq. (3) is characteristic for any type of interaction in a highly excited atom when this interaction is significant in a region of the order of the dimensions of the atomic core. As an example, Fig. 1 shows the experimental dependence on the principal quantum number of the doublet splitting for the  $D_{3/2} - D_{5/2}$  levels of a highly excited sodium atom.<sup>20, 21</sup> The fine structure splitting of the levels is determined by the inner region of the atomic core, so that the quantity  $A = n^3 \delta W_n$  ( $\delta W_n$  is the fine structure splitting of the levels) does not depend on  $n$  for large values of  $n$ . This behavior is shown in Fig. 1, where the quantity  $A$  is expressed in units of  $10^{10} \text{ cm}^{-1}$ .

## 2. PRODUCTION OF ATOMS IN RYDBERG STATES

Let us examine the experimental methods for obtaining highly excited atoms. These methods make use of three types of processes: electron impact excitation of atoms and molecules, charge exchange of ions with atoms and molecules, and photoexcitation. The first two methods for obtaining highly excited atoms, namely, the process of charge exchange of ions with atoms and molecules<sup>9, 10, 22-33</sup> and the process of electron impact ex-

<sup>2)</sup>In order to simplify the notation, in future we will not distinguish between the principal quantum number  $n$  and the effective principal quantum number  $n^*$  because these quantities become equal for  $n \rightarrow \infty$ . Thus, when the principal quantum number  $n$  is used to characterize the binding energy of an excited electron, a more rigorous analysis would require that  $n$  be replaced by  $n^*$ .

TABLE III. Maximum values of  $\sigma(E)$ , the cross section for electron impact excitation of inert gas atoms ( $E_{\max}$  denotes the electron energy at which the maximum is attained).

Atom	He	Ne	Ar	Kr	Xe
$\sigma(E_{\max}), \text{\AA}^2$	0.77	0.63	6.5	4.0	10
$E_{\max}, \text{eV}$	70	60	28	20	20

citation of atoms and molecules,<sup>34-43</sup> as well as the process of molecular dissociation by electron impact with the formation of highly excited atoms,<sup>44-50</sup> were widely used in the early studies of atoms in Rydberg states. The disadvantage in these methods is that they lead to the formation of an entire spectrum of highly excited atomic states. At the same time, the cross section for producing atoms with a given value of the principal quantum number  $n \gg 1$  is described by the following function:

$$\sigma_n(E) = \frac{\sigma(E)}{n^3}, \quad (5)$$

where  $\sigma(E)$  does not depend on the principal quantum number of the state.

The function (5) is easy to obtain taking into account the fact that the interactions and transitions occur in a region that is small in comparison with the size of the Rydberg atom. The probability of the transition equals

$$w_{0 \rightarrow n} = |\langle \Psi(R = \infty) - \psi_0 | \psi_n \rangle|^2,$$

where  $\psi_0$  and  $\psi_n$  are the wave functions of the atom in the initial and final states;  $\Psi(\mathbf{R})$  is the exact wave function of the system, where  $\mathbf{R}$  is the distance vector between the nucleus and the incident particle. Since the interaction with the incident particle occurs over a limited range of electron coordinates, the change in the wave function of the system  $\Psi - \psi_0$  occurs only in this region. The wave function of a highly excited electron varies as  $\psi_n \sim n^{-3/2}$  near the nucleus. From this we obtain the function (5).

Tables III and IV show the values of  $\sigma(E)$  in Eq. (5) for electron impact excitation of inert gas atoms. These quantities were measured in Ref. 42.

Only optical methods allow production of Rydberg atoms in a selected state. Existing methods for selective excitation of atomic Rydberg states depend on the use of tunable lasers. The advent of tunable lasers opened up new possibilities for selective excitation of atomic Rydberg states and raised the study of Rydberg states to a new scientific level. At the present time, tunable lasers in combination with nonlinear crystals allow obtaining laser radiation that can be smoothly tuned over a frequency range from 2,000 to 30,000  $\text{\AA}$  (photon energy ranging from 6 to 0.4 eV, respectively).

There exist various methods for laser excitation of atomic Rydberg states. The simplest of these is single-photon excitation, involving the excitation of a Rydberg state by absorption of a single photon. An example of this method of excitation is the work described in Refs.

TABLE IV. Value of  $\sigma(E)$  for an electron with incident energy of 100 eV.

Atom	He	Ne	Ar	Kr	Xe
$\sigma(E), \text{\AA}^2$	0.67	0.61	1.5	2.0	4.6

51-53, where helium atoms in  $n^3P(n=8-17)$  states were produced by exciting metastable helium atoms  $\text{He}(2^3S)$  with a tunable laser using a frequency doubling ADP crystal (ammonium diphosphate). As a result, the laser wavelength varied over a range from 2,723 to 2,626  $\text{\AA}$ . Metastable helium atoms were produced in a gas discharge. Measurements were performed on the afterglow of the gas discharge. Other examples of this type of excitation are the excitation of  $np$ -states of rubidium atoms with principal quantum numbers in the range  $n=28-60$  (Ref. 54) and the excitation of  $np$ -states of cesium atoms for  $n=28-78$  (Ref. 55).

Another method for laser excitation of Rydberg states makes use of two-photon excitation, when resonant excitation of a given state involves simultaneous absorption of two photons (see, for example, Refs. 56-59). In contrast to single-photon spectroscopy, two-photon laser spectroscopy permits studying other excited states with a change in orbital angular momentum of the electron  $\Delta l = 0, 2$ . It would seem that the two-photon excitation method is much less effective than the single-photon method because the coefficient for two-photon absorption contains an additional small parameter that depends on the ratio of the intensity of the electromagnetic field to the characteristic magnitude of the atomic field. However, in spite of this, two-photon laser spectroscopy has important advantages over single-photon processes. The single-photon absorption coefficient increases in proportion to the decrease in the laser line width and reaches saturation when this width becomes equal to the Doppler width. Thus, single-photon laser spectroscopy permits studying the structure of the absorption coefficient over a range of the order of the Doppler width of the spectral line.

A different situation arises in two-photon laser spectroscopy. In the usual experimental setup, the incident radiation turns out to be partially trapped in the region between two parallel mirrors. For this reason, two photons moving in opposite directions are usually absorbed so that the Doppler effect is eliminated. Evidently, the advantages of two-photon laser spectroscopy become apparent when the laser line width is small in comparison with the Doppler width. First of all, the two-photon absorption coefficient increases in proportion to the decrease in the laser intensity, while the single-photon absorption coefficient becomes saturated at these intensities. Thus, the relative efficiency of two-photon laser spectroscopy increases as the laser line width decreases. Second, two-photon laser spectroscopy allows studying the fine structure of the absorption spectrum, the scale of which is characterized by the width of the laser line. The resolution of single-photon laser spectroscopy is determined by the Doppler width of the line.

We note that the methods examined above, which make use of a tunable laser, lead to the production of highly excited atoms with low electron orbital angular momentum. This follows from the selection rules for photon absorption. According to these rules, for allowed transitions, single-photon absorption changes the electron orbital angular momentum by not more than one unit. In order to obtain atoms with high orbital angular momentum, it is necessary to use a strong electromagnetic field. When the intensity of the field is high enough, states with different values of the electron orbital angular momentum are mixed so that the excited state is characterized by the parabolic quantum numbers  $n$ ,  $n_1$ ,  $n_2$ , and  $m$ . In this case, the atomic energy levels are split by the field so that tuning over the resonance region can be performed by changing the intensity of the electrostatic field while keeping the laser frequency constant.

We will describe some of the details of the experiment performed by Koch, who suggested and developed this method.<sup>60,61</sup> A beam of 7.51 keV protons undergoes charge exchange with xenon atoms and then passes through two regions between capacitor plates with constant electric fields  $F_1$  and  $F_2$ . In these regions, the hydrogen atoms are excited by the  $R=22$  line radiation from a carbon dioxide laser. The initial distribution of hydrogen atoms among the atomic states satisfies  $f_n \sim n^{-3}$ . In the first capacitor, the field intensity is of the order of tens of kV/cm and in this capacitor excitation occurs as a result of a transition from  $n=7$  to  $n=10$ . In the second capacitor, the intensity of the electric field is of the order of hundreds of V/cm and in this region transitions from  $n=10$  to  $n=31$  occur.

According to calculations, in the first capacitor with an electric field intensity  $F_1=42.56$  kV/cm, resonance occurs for the transitions  $7, 2, 4, 0 \rightarrow 10, 1, 8, 0$  while with a field intensity  $F_1=42.62$  kV/cm, the absorption of a laser photon corresponds to the transitions  $7, 1, 3, 2 \rightarrow 10, 0, 7, 2$ . Evidently, in order to detect atoms in sharply defined states, high precision is required for the intensity of the electric field, which in the published literature amounts to  $\Delta F/F \sim 10^{-3}$ ; future plans call for lowering this ratio to  $10^{-5}$ . In the second capacitor, the electric field of the laser, which is characterized by an electric field intensity equal to 90 V/cm at a laser intensity of 20 W/cm<sup>2</sup>, contributes to the splitting of the levels.

Thus, the method examined above, which is intended for producing highly excited atoms with arbitrary orbital angular momentum, requires highly stable external fields. When using a constant electric field in a capacitor, it is ultimately possible to obtain atoms in states with  $n \sim 25-30$ , while with an alternating electromagnetic field in the capacitor the range of values of  $n$  is increased to  $n \sim 70$ .

Later on, we will consider the problem of estimating how many highly excited states can be produced with the aid of a tunable laser. Since the absorption efficiency drops sharply with increasing principal quantum number, we will concentrate on single-photon laser spectroscopy. At the same time, we will assume that the

laser line is sufficiently narrow and the gas or atomic beam is sufficiently rarefied so that the width of the absorption line is determined by the Doppler broadening mechanism. Selective excitation of particular states occurs when the width of the absorption line is much smaller than the distance between neighboring levels. In the case being examined, the width of the Doppler broadened line is  $\Delta\omega \sim \omega_0 v_T/c$ , where  $\omega_0$  is the transition frequency at the center of the line,  $v_T$  is the thermal speed of the atoms,  $c$  is the speed of light, and the distance between neighboring levels is of the order of  $\omega_0/n^3$ . From this, we find that under the conditions considered the possibility of selective excitation of a Rydberg level is determined by

$$n^3 \ll \frac{c}{v_T}. \quad (6)$$

Let us make some numerical estimates. The quantity  $c/v_T$  is of the order of  $10^6$  (the temperature of the gas or the longitudinal temperature of the atoms in the beam is assumed to be of the order of room temperature). This gives  $n < 100$ , i.e., it is possible to excite a level with principal quantum number less than 100. We note that in making this estimate we assumed that the gas or the beam of atoms is sufficiently rarefied so that impact broadening of the spectral line is not important.

Let us estimate the excitation selectivity due to the instability in the wavelength of the tunable laser. For a tunable dye laser, the line width together with its instability usually constitutes several tenths of cm<sup>-1</sup>. Assuming that this quantity, which we will denote by  $\Delta E$ , lies in the range from 0.1 cm<sup>-1</sup> to 1 cm<sup>-1</sup>, we can determine the limiting value of the principal quantum number  $n$  for a selectively excited atomic Rydberg state from the relation

$$\Delta E = \frac{1}{n^3}. \quad (7)$$

Here,  $1/n^3$  is the difference of the excitation energy for the states with principal quantum numbers  $n$  and  $n+1$  expressed in atomic units. From this relation we find that under the given conditions the limiting values of the principal quantum number for selectively excited atomic Rydberg states lie in the range  $n=60-130$ .

The estimates made above show that with the help of a tunable laser it is possible to excite selected atomic Rydberg states up to  $n \sim 100$ . In making these estimates we assumed a dye laser, i.e., we assumed that the photons that excite this state lie in the visible and adjacent, parts of the spectrum, while the width of the laser line likewise corresponds to that of a tunable dye laser. The experimental methods described above allow selective production of atoms in Rydberg states with  $n \leq 100$ . However, this limit on the principal quantum number is not a fundamental limit. It is possible to change the method of producing atomic Rydberg states by carrying out the excitation in steps so that the last step is an excitation from a Rydberg state with principal quantum number  $n' \leq 100$ . Then, the conditions (6) and (7) become less severe. Condition (6) in this case has the form

$$n \ll \left( \frac{c}{v_T} n'^2 \right)^{1/3}. \quad (8)$$

where  $n$  is the principal quantum number of the final Rydberg state. Evidently, in the scheme under consideration, Doppler broadening of spectral lines does not prohibit selective production of atomic Rydberg states with  $n \lesssim 10^3$ . Condition (7) in this case takes the form

$$\frac{\Delta\omega}{\omega} \sim \frac{n'^2}{n^3}. \quad (9)$$

For  $n' \sim 10^2$  and  $n \sim 10^3$ , this formula yields  $\Delta\omega/\omega \sim 10^{-5}$ .

The theoretical estimates obtained above for the limiting values of the principal quantum number of selectively detected Rydberg atoms cannot be achieved experimentally. Indeed, according to these estimates Rydberg atoms with  $n \sim 10^3$  can be selectively produced by exciting states with  $n' \sim 100$ . This can be achieved by using a tunable laser in the centimeter wavelength range with a relative line width  $\Delta\omega/\omega \sim 10^{-5}$ , which is presently impossible to attain. Nevertheless, the scheme described above allows increasing the range of principal quantum numbers for selectively excited Rydberg states. If a  $10.6 \mu\text{m}$  tunable carbon dioxide laser is used at the last stage of excitation, which corresponds to  $n' = 11$ , then the limit due to the Doppler broadening of the line in accordance with the condition (8) corresponds to  $n \sim 500$ . According to (9), for such values of the principal quantum number, the laser line width must satisfy the criterion  $\Delta\omega/\omega \sim 10^{-6}$ . These conditions can be satisfied by using modern experimental techniques.

Production of atoms with high principal quantum numbers, as well as the possibility for studying processes involving these atoms and for using these states for other purposes, depend on the efficiency of the photo-processes that lead to the formation or destruction of highly excited atoms. For this reason, these processes will be examined below.

### 3. RADIATIVE TRANSITIONS OF HIGHLY EXCITED ATOMS

Let us study the production of highly excited atoms by photoprocesses, as well as photon absorption and emission by highly excited atoms. Studying these processes will permit us to evaluate the potential for producing highly excited atoms in selected states, as well as the possibility of using them for various studies.

Let us first determine the cross section for photo-excitation of an atom into a given Rydberg state in order to identify the highly excited atomic states that can be selectively produced under real conditions. To do so, we will make use of the similarity of the process of photoexcitation of an atom into a Rydberg state and the process of photoionization of an atom near the threshold. These processes are characterized by the same interaction mechanism for the transition, which is determined by a region of the order of the dimensions of the atom in the initial state and differ only in that, in the former case, the electron makes a transition into a discrete state, while in the latter case it makes a transition into the continuous spectrum. This defines a simple relationship between the cross sec-

tions for these processes. In particular, if the width of the absorption line significantly exceeds the distance between neighboring energy levels of the Rydberg atom, then the absorption cross section in the discrete spectrum coincides with the cross section for photoionization of the atom. Using the analogy between these processes, we will establish below a relationship between the corresponding cross-sections (see also Ref. 43).

We will make use of the fact that the oscillator strength for exciting high-lying electron bound states with principal quantum number  $n$  varies as  $n^{-3}$  (see, for example, Ref. 16). This allows writing the excitation cross section in the following form:

$$\sigma_n = \frac{C}{n^3} a(\omega - \omega_n), \quad (10)$$

where  $C$  is a normalization constant, while  $a(\omega - \omega_n)$  is a function that characterizes the shape of the spectral line in absorption. This function is normalized to unity  $\int a d\omega = 1$ , and its value depends only on the difference in the frequency of the exciting photons  $\omega$  and the frequency corresponding to the transition to the line center  $\omega_n$ . On the scale of frequencies for atomic transitions, this function is a delta function  $a = \delta(\omega - \omega_n)$ . The width of the distribution function is determined by the broadening mechanism (see, for example, Ref. 62).

We will begin with the fact that for large widths of the absorption line, significantly exceeding the distance between levels with different values of  $n$ , the cross section for photon absorption coincides with the cross section for photoionization near threshold. Indeed, in this case, the discrete spectrum of the excited electron is sensed by the photon as a continuous spectrum, while the behavior of a weakly bound and that of a slow free electron are identical near the atomic core. Therefore we have:

$$\sigma_{\text{ion}} = \sum_n \sigma_n = \sum_n \frac{C}{n^3} a(\omega - \omega_n). \quad (11)$$

In this case,  $\sigma_{\text{ion}}$  includes that part of the photoionization cross section that corresponds to the formation of a slow electron with the same orbital angular momentum (or with the same parity) as the excited electron.

Let us determine the normalization constant in Eq. (10). Under the conditions considered, the sum in Eq. (11) can be replaced by an integral. Further, the energy of the atomic transition under consideration equals

$$\omega_n = J - \frac{1}{2n^2},$$

where  $J$  is the ionization potential of the atom. From this we obtain

$$\sigma_{\text{ion}} = C \int \frac{dn}{n^3} a\left(\omega - J + \frac{1}{2n^2}\right).$$

Using the normalization condition for the distribution function  $\int a(x) dx = 1$ , we obtain  $\sigma_{\text{ion}} = C$ , so that

$$\sigma_n = \frac{\sigma_{\text{ion}}}{n^3} a(\omega - \omega_n). \quad (12)$$

In deriving this formula<sup>3)</sup>, we used the assumption

<sup>3)</sup>A general relation was obtained in Ref. 43 relating the cross section for exciting an atom into a highly excited state and the ionization cross section of the atom near the threshold for an arbitrary process. In the case being considered, this relation has the form  $\int \sigma_n d\omega = \sigma_{\text{ion}}/n^3$ .

that  $\Delta\omega \ll 1/n^2$ , where  $\Delta\omega$  is the absorption line width, because we assumed that only discrete atomic states are involved in the process of absorbing photons with a given frequency. However, the formula obtained is also valid when this condition is not satisfied.

Equation (12) can be represented in a form that is more specific and more convenient for analysis if the lower state of the atom has a quantum number  $n' \gg 1$ . In this case, we can obtain a simple expression for the excitation cross section using Kramer's formula<sup>63</sup> for the photoionization cross section of an excited atom

$$\sigma_{\text{ion}} = \frac{16\pi}{3} \sqrt{\frac{1}{3}} \frac{1}{cn'^5\omega^3}; \quad (13)$$

where  $c = 137$  is the speed of light and  $\omega = 1/2n'^2 - 1/2n^2$  is the energy of the absorbed photon. Eq. (9) represents the classical ionization cross section for the electron, averaged with respect to the angular momentum and its projection along a fixed axis. It is valid if  $n - n' \gg 1$  so that the classical description of the electron undergoing the transition is valid. Taking into account (13), Eq. (12) can be represented in the form

$$\sigma(n' \rightarrow n) = \frac{128\pi}{3} \sqrt{\frac{1}{3}} \frac{n'}{n^3} \left(1 - \frac{n'^2}{n^2}\right)^{-3} a(\omega - \omega_n) = \frac{0.565n'}{n^3} \left(1 - \frac{n'^2}{n^2}\right)^{-3} a(\omega - \omega_n). \quad (14)$$

Under actual conditions for producing atomic Rydberg states, the density of atoms is not large so that the spectral lines are broadened according to the Doppler mechanism. In this case, the distribution function  $a(\omega - \omega_n)$  at the line center equals  $a(0) = 1/\omega\sqrt{Mc^2/2\pi T}$ , where  $\omega$  is the frequency of the absorbed photon,  $M$  is the mass of the atomic nucleus,  $c$  is the speed of light, and  $T$  is the temperature of the gas. Substituting this expression into Eq. (14), we obtain the following expression for the cross section for the phototransition under consideration at the line center:

$$\sigma(n' \rightarrow n) = 1.13 \left(\frac{n'}{n}\right)^3 \left(1 - \frac{n'^2}{n^2}\right)^{-3} \sqrt{\frac{Mc^2}{2\pi T}}. \quad (15)$$

In particular, for  $n = 2n'$  and  $T = 273$  K, this formula yields  $\sigma(n' \rightarrow n) = \sigma_0\sqrt{M}$ , where  $M$  is the mass of the nucleus expressed in atomic mass units, while  $\sigma_0 = 10^{-12}$  cm<sup>2</sup>. We note that under the conditions being considered the cross section for photoionization of the atom in the  $n$ -th state by the same photon, according to formula (13), equals  $\sigma_{\text{ion}} = \sigma'n$ , where  $\sigma' = 1.9 \cdot 10^{-17}$  cm<sup>2</sup>. Since, realistically,  $n \leq 10^2$ , the ionization cross section for the highly excited atom is about three orders of magnitude lower than the cross section for photoexcitation of the atom into a given level. Thus, highly excited atoms created as a result of laser excitation do not disintegrate under the action of such laser radiation.

Another estimate, based on the formulas presented for the excitation cross section, enables us to understand what fraction of the atoms in the lower state  $n'$  can be put into the highly excited state  $n$ . We will assume in accordance with the estimates made that the cross section for photoexcitation into the  $n$ -th state is of the order of  $\sigma \sim 10^{-12}$  cm<sup>2</sup>. Let the beam of atoms move with a speed of the order of the thermal speed  $v \sim 10^5$  cm/s and let the length of the path irradiated by

the laser be  $l \sim 1$  cm. Then, each atom in the state  $n'$  that enters this zone is excited with a probability of the order of unity if the flux of laser photons amounts to  $j \sim v/l\sigma \sim 10^{17}$  1/cm<sup>2</sup>·s. This requires a tunable laser power  $P \sim 0.1$  W/cm<sup>2</sup>, which corresponds to real tunable dye lasers.

Let us examine the situation in which the laser pulse used for pumping is of duration that is short in comparison with the transit time of the atom in the irradiation zone (10 ms under the conditions considered). The atom in the lower state  $n'$  will be excited into the state  $n$  with a probability of the order of unity if the number of photons per unit surface area is of the order of  $1/\sigma \sim 10^{12}$  cm<sup>-2</sup>. This corresponds to a laser pulse intensity of the order of  $10^{-6}$  J/cm<sup>2</sup>. Such intensities are easily attainable. Thus, we conclude that by using modern laser technology we can selectively populate a highly excited state by exciting a significant fraction of the atoms in the lower state. In this manner, the existing laser technology allows selective production of highly excited atomic states with a relatively high density of atoms in a given state.<sup>4)</sup> The high efficiency of modern methods for detecting atoms in selected Rydberg states has led to great progress in studying processes that involve highly excited atoms.

Another type of radiative transition out of Rydberg states, which we will examine below, is responsible for the radiative lifetime of highly excited atoms. This quantity is determined by radiative transitions into lower states and varies as  $n^3$  with increasing excitation. For this reason, the radiative lifetime of highly excited states is long and they can be considered as metastable states. In addition, the radiative lifetime of a highly excited state sharply increases with increasing orbital angular momentum. In order to represent the order of magnitude of the radiative lifetimes of highly excited states, we will present below the values of the frequencies of the most intense radiative transitions out of a highly excited state for hydrogen atoms.

The most effective such radiative transition out of the state  $nl$  is the transition into the state  $n'l, l' = l - 1$ .

This transition makes the greatest contribution to the radiative lifetime of a highly excited state. The probability of such a transition per unit time, according to general formulas for the radiative transitions in the hydrogen atom,<sup>16,64</sup> equals

$$A(nl \rightarrow l, l-1) = \frac{16}{3c^3} \frac{(n+l-1)!}{(n-l)!(2l+1)!} \frac{(n-l)^{2n-2l} (4nl)^{2l}}{(n+l)^{2n+2l}}. \quad (16)$$

Here,  $A$  is the Einstein coefficient for the transition under consideration from the upper into the lower state expressed in atomic units and averaged with respect to the magnetic quantum number of the electron, while  $c$  is the speed of light. It is convenient to compare the quantity sought with the probability of a radiative transi-

<sup>4)</sup>Under the examined conditions, the density of highly excited atoms in a given state per unit length of the beam attains  $10^{12}$  cm<sup>-2</sup>, which for a cell length  $l \sim 1$  cm illuminated by the laser corresponds to a density of excited atoms of the order of  $10^{12}$  cm<sup>-3</sup>.

TABLE V. Values of the reduced probability of a radiative transition per unit time for different values of the orbital angular momentum for  $l \ll n$ .

$l$	1	2	3	4	5
$n^3 \frac{A(nl \rightarrow l, l-1)}{A(21 \rightarrow 10)}$	6.08	1.56	0.498	0.182	0.0723

tion per unit time for the  $2p$ -state of the hydrogen atom, i.e., with the quantity  $A_0 = A(21 \rightarrow 10) = 6.27 \cdot 10^8 \text{ s}^{-1}$ . Using this property, we can represent Eq. (16) for  $l \ll n$  as follows:

$$A(nl \rightarrow l, l-1) = \frac{A_0}{n^3} \frac{3^l}{2^l} \frac{e^{-l} (4l)^{2l}}{(2l+1)!}. \quad (17)$$

Table V includes calculations based on this formula for small values of orbital angular momentum.<sup>5)</sup> As can be seen, the radiative lifetime decreases sharply with increasing orbital angular momentum.

The analysis presented above allows an estimate to be made of the order of magnitude of the radiative lifetimes for highly excited atoms<sup>6)</sup> and of their dependence on the quantum numbers. For  $n \sim 50$ , the radiative lifetime  $\tau \sim 10^{-5} \text{ s}$  so that in the beam method for producing highly excited atoms this quantity significantly exceeds the residence time of the highly excited atoms in the zone being studied.

Of particular interest are the radiative transitions between highly excited states. The oscillator strength for the transition  $nl \rightarrow n'l'$  for  $n, n' \gg 1$  is given by the expression<sup>65,66</sup>

$$f(nl \rightarrow n', l \pm 1) = \frac{n_c}{3s} \left[ J_s'(e_s) \pm \frac{l_c}{\sqrt{n_c^2 - l_c^2}} J_s(e_s) \right]^2, \quad (18)$$

where  $s = n - n'$ ,  $n_c = 2m'/(n + n')$ ,  $l_c = \max(l, l')$ ,  $\varepsilon = 1 - (l_c^2/n_c^2)$ , and  $J_s$  is a Bessel function. Due to the unwieldy nature of this expression, we will limit ourselves to transitions between neighboring levels. In this case, we have for  $l \ll n$ :

$$A(n, l \rightarrow n-1, l \pm 1) = \frac{1.84}{n^3} A_0, \quad (19)$$

where  $A_0 = A(2p \rightarrow 1s) = 6.27 \cdot 10^8 \text{ s}^{-1}$ .

Comparing Eq. (19) with Eq. (17), we find that radiative transitions from highly excited state to neighboring levels make a small contribution ( $\sim 1/n^2$ ) to the radiative

<sup>5)</sup> For  $l \gg 1$ , the dependence on  $l$  has the form

$$A(nl \rightarrow l, l-1) \sim \frac{1}{n^3} \left( \frac{2}{e} \right)^l l^{-3/2}.$$

<sup>6)</sup> We note that although a radiative transition to a lower state makes a large contribution to the radiative lifetime of the highly excited state, this transition does not determine the radiative lifetime. Thus, for the transition  $np \rightarrow n's$ , the Einstein coefficients  $A(n1 \rightarrow n'0)$  for transitions to the final states  $1s, 2s, 3s, 4s$  have the ratios  $1:0.58:0.43:0.46$ , while for the transition  $nd \rightarrow n'p'$  with final states  $2p, 3p, 4p$  the ratios are  $1:0.82:0.69$ . Thus, Eqs. (16) and (17) can be used only for estimating the radiative lifetime of a highly excited state and for determining its dependence on the parameters of the state.

lifetime of an atomic Rydberg state. However, such transitions can be used for obtaining long wavelength radiation. In order to evaluate the possibilities for a maser generating radiation in such transitions, let us determine the cross section for absorbing a photon in making the transition under consideration:

$$\sigma_{\text{abs}} = \frac{\pi^2 c^2}{\omega^3} a(\omega - \omega_0) A(nl \rightarrow n', l \pm 1).$$

We will assume that the levels are hydrogen-like, i.e. the frequency at the line center is  $\omega_0 = 1/n^3$  in accordance with Eq. (2), while the broadening is Doppler-like so that, as in Eq. (15), the photon distribution function at the line center is given by  $a(0) = 1/\omega_0 \sqrt{Mc^2/2\pi T}$ , where  $M$  is the mass of the nucleus of the excited atom and  $T$  is the temperature of the gas. Then, based on Eq. (19), we obtain

$$\sigma_{\text{abs}} = 1.08 \cdot 10^{-14} \text{ cm}^2 \cdot n^4 \sqrt{M}. \quad (20)$$

where the mass of the nucleus  $M$  is expressed in atomic mass units. Table VI displays the parameters for the radiative transitions being examined: the position of the level  $n$  that yields the assigned wavelength for transitions between neighboring levels and the parameters of these transitions.

Analysis of Table VI shows the convenience of using highly excited atomic states as sources of monochromatic long wavelength radiation. Masers based on them have many advantages over existing hydrogen and rubidium masers. These advantages are connected with the fact that in this case allowed transitions are used while in existing masers a strongly forbidden transition is used. For this reason, in the case being considered, we have a large photon absorption cross section and a high amplification factor, which makes it much easier to generate laser radiation. In addition, many transitions are available, and therefore, there are many possibilities for generating laser radiation.

In order to demonstrate these possibilities, the characteristics of the radiative transitions  $nl \rightarrow n, l+1$  are displayed in Table VII. As is evident from Table VI, it is difficult to generate radiation in the centimeter wavelength region because it is difficult to selectively produce atoms in states with  $n \geq 100$ . Thus, for this purpose, it is convenient to use the transitions  $nl \rightarrow n, l \pm 1$ , which will yield these wavelengths for relatively small values of the principal quantum number  $n$ . The transition frequency in atomic units constitutes  $(\sigma_l - \sigma_{l+1})/n^3$ ; the width of the emission and absorption line for such a transition is determined by the radiative lifetime, which is determined from Eq. (16). The values of the quantum

TABLE VI. Characteristics of radiative transitions between neighboring levels ( $n \rightarrow n-1$ ) of atoms in Rydberg states.

photon wavelength, cm	0.01	0.1	1	10
$n$	13	28	60	130
$A(nl \rightarrow n-1, l \pm 1), \text{ s}^{-1}$	$3.0 \cdot 10^3$	66	1.4	0.03
$\sigma_{\text{abs}}/\sqrt{M}, \text{ cm}^2$	$3.1 \cdot 10^{-10}$	$6.6 \cdot 10^{-9}$	$1.4 \cdot 10^{-7}$	$3.1 \cdot 10^{-6}$

TABLE VII. Radiative properties of the transition  $nf \rightarrow nd$ .

$n$	10	15	20	25	30	35	40
Photon wavelength, cm	1.5	5.0	11.8	23	40	63	94
Radiative lifetime of $d$ -state, s	$3.2 \cdot 10^{-6}$	$1.1 \cdot 10^{-5}$	$2.6 \cdot 10^{-5}$	$5 \cdot 10^{-5}$	$8.7 \cdot 10^{-5}$	$1.4 \cdot 10^{-4}$	$2.0 \cdot 10^{-4}$
$A(nf \rightarrow nd), s^{-1}$	$6.2 \cdot 10^{-3}$	$8.1 \cdot 10^{-4}$	$1.9 \cdot 10^{-4}$	$6.3 \cdot 10^{-5}$	$2.5 \cdot 10^{-5}$	$1.2 \cdot 10^{-5}$	$6.0 \cdot 10^{-6}$
$\sigma_{\text{abs}}, \text{cm}^2$	$6.8 \cdot 10^{-9}$	$3.4 \cdot 10^{-8}$	$1.1 \cdot 10^{-7}$	$2.5 \cdot 10^{-7}$	$5.5 \cdot 10^{-7}$	$1.0 \cdot 10^{-6}$	$1.7 \cdot 10^{-6}$

defects of the  $d$ - and  $f$ -states in Table VII were taken from Table I and correspond to an excited helium atom.

Analysis of Table VII demonstrates the large photon absorption and emission cross sections, which are determined by the effectiveness of the radiative transition used. For comparison, we point out the fact that the frequency of a radiative transition between the components of the hyperfine levels of the hydrogen atom at a wavelength of 21 cm, which is used in the hydrogen maser, constitutes  $2.8 \cdot 10^{-15} \text{ s}^{-1}$ . According to Table VII, the allowed transition at this wavelength between highly excited states of the atom precedes ten orders of magnitude more quickly. The high photon emission cross section, and therefore, the high amplification factor, makes it easy to generate laser radiation in the system under consideration, which operates in the superradiant mode. Further, the power of the masers being considered can be estimated from the formula  $P\lambda_0/\lambda_m$ , where  $P$  and  $\lambda_0$  are the power and wavelength of the tunable laser, while  $\lambda_m$  is the wavelength of the maser. The maser power estimated according to this formula amounts to  $10^{-5}$ – $10^{-6}$  W in the centimeter wavelength range, while the power of the rubidium maser operating on the forbidden transition between hyperfine states turns out to be of the order of  $10^{-10}$  W. Finally, the possibility for choosing different transitions and the possibility for tuning them in an external electric or magnetic field makes the maser being considered a very convenient source of long wavelength radiation. With all the advantages of this kind of maser, it should be noted that the wavelength stability of the generated radiation cannot compete with the stability of the hydrogen maser.

#### 4. METHODS FOR DETECTING ATOMS IN RYDBERG STATES

Atoms in Rydberg states are produced in order to study their properties and mainly for studying various reactions in which they participate. For this reason, an important aspect of studying atoms in Rydberg states is developing reliable methods for detecting such atoms. There are three methods for detecting excited atoms. One of these methods is related to the measurement of the intensity of line radiation resulting from radiative decay of the excited atom (see, for example, Refs. 51–53, 58). Two other methods rely on ionization of the highly excited atom followed by detection of the ion formed. The first of these methods makes use of ionization of atoms in Rydberg states near metallic surfaces, while the second method involves ionization in an external electric field. Below, we will analyze each of these methods for detecting atoms in

Rydberg states.

Highly excited atoms are detected by their fluorescence only for small values of the principal quantum number. This is due to the fact that the lifetime of the excited states increases sharply with excitation ( $\sim n^3$  for states with small orbital angular momentum) so that the intensity of the radiation drops sharply with increasing excitation. In addition, the intensity of the fluorescence itself is small, which affects the sensitivity of the method. As an example of the most complete exploitation of this method for detecting highly excited atoms we present the data from Ref. 58, where in the two-photon absorption spectrum for the transition  $5s - 32d$  was measured using the fluorescence of excited rubidium atoms. The fluorescence involving transitions  $np - 5s$  ( $n \geq 6$ ) was measured for the rubidium atom in the wavelength range 3,800–4,800 Å. It resulted from the steplike photodecay of highly excited  $nd$ -rubidium atoms. The intensity of the fluorescence signal decreased with increasing excitation as  $n^{-(4.2 \pm 0.6)}$ . Such a sharp drop in sensitivity limits the usefulness of the method for large values of the principal quantum number. For this reason, highly excited atoms are usually detected by the ion current formed when such atoms are ionized.

Other methods for detecting highly excited atoms depend on the detection of ions when such atoms are ionized. Various methods are used for ionizing highly excited atoms for the purpose of their detection. One such method involves ionization of highly excited atoms on collision with atoms or molecules.<sup>34,35</sup> A second method for detecting highly excited atoms is based on the disintegration of such atoms near metallic surfaces.<sup>35,36,50,67,69</sup> The ionization of highly excited atoms near metallic surfaces is related to charge exchange at the metallic surface, accompanied by escape of the electron into the metal. During a collision of a highly excited atom with a metallic surface, this process occurs with a probability of unity.<sup>70</sup>

A very sensitive method for detecting highly excited atoms is based on the use of a thermionic detector.<sup>37,43,56,57,59,68</sup> In this technique, excited atoms are ionized near a heated cathode as a result of collisions with electrons. Subsequently, the ions penetrate into the space charge region of the diode and influence the diode current. This method has a high sensitivity,<sup>56,57,59,69</sup> yielding an ion amplification coefficient of the order of  $10^5$ . In particular, in Ref. 59, this method allowed detecting highly excited rubidium atoms up to  $n = 85$ .

A disadvantage of the methods for detecting highly excited atoms based on their ionization as a result of collisions with atoms and molecules or as a result of ionization near a heated cathode is the lack of selectivity. These methods allow detecting atoms with different values of the principal quantum number with the same sensitivity, beginning with some principal quantum number. The same situation occurs when highly excited atoms pass through a metallic grid. Depending on the dimensions of the grid cells, this method allows detecting highly excited atoms with identical sensitivity, beginning with a particular principal quantum number.

In this respect, the most attractive method of detection relies on ionization in a constant uniform electric field. This method has been most widely used in recent times. As a result, we will examine below the physics of this process.

The ionization process for an atom in a constant electric field is connected with a sub-barrier transition of the electron into the classical region of electron motion (Fig. 2). The initial experimental<sup>71</sup> and theoretical<sup>72,73</sup> studies of this process were carried out in connection with the disappearance of the visible lines of atoms with increasing intensity of the electric field into which the fluorescing gas has been placed. This occurs as a result of the disintegration of the excited atoms in the electric field. For this reason, excited atoms that emit photons in the absence of an electric field and make a transition into a lower state are ionized in an electric field, and this is what causes the disappearance of the corresponding visible lines. Later on, this process was repeatedly used as a method for ionizing excited atoms. For this reason, this process has been repeatedly examined in reviews and monographs (see, for example, Refs. 74-77).

The theory of the ionization of an atom in a constant electric field is based on asymptotic considerations,<sup>78,79</sup> according to which the time for the sub-barrier transition of an electron into the continuous spectrum is short in comparison with the characteristic electron times. In this case, the classically accessible region of the electron motion is separated from the region over which the field of the atomic core acts by a fairly wide barrier, so that the frequency of the electron leaking through the barrier decreases exponentially with decreasing field intensity. Unfortunately, the known ionizing transitions<sup>77</sup> involve a barrier width that significantly exceeds the dimensions of the atom. This occurs for weakly excited atoms or for a negative ion. For ionization of highly excited atoms, electric field intensities for which the barrier width is comparable with the dimensions of the electron orbit are of interest.

Let us determine the parameters for the disintegration of a highly excited atom as a function of the electric field intensity. The potential, in which the electron moves is given by

$$U = -\frac{1}{r} - Fz, \quad (21)$$

where  $r$  is the distance between the electron and the atomic core,  $z$  is the coordinate along the electric field, and  $F$  is the intensity of the electric field. The ionization potential of the atom equals  $-\epsilon = 1/2n^2$ , where  $n$  is the principal quantum number. Evidently, for an electric field intensity<sup>71</sup>

$$F_0 = \frac{1}{16n^4} \quad (22)$$

the barrier vanishes at a point  $z_0 = 4n^2$  on the axis. The

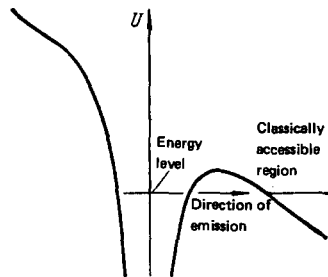


FIG. 2. Profile of the potential in which the electron moves when an excited atom is ionized in an electric field.

region of action of the atomic core potential and the classically allowed region of electron motion come into contact at this point. For  $F < F_0$ , these regions separate.

However, Eq. (22), which has been widely used, is incorrect. It does not take into account the real geometry of the system, as well as the shift in the energy level of the electron due to the action of the field. The electric field intensity at which the level is expected to emerge into the continuous spectrum depends on the parabolic quantum numbers of the state  $n_1, n_2$ . For the state  $n_1 = n$ , for which the electron orbit has maximum elongation along the direction of decreasing electric field, the electric field depresses the energy level of the electron. For this reason, this level emerges into the continuous spectrum at a higher field than that indicated by Eq. (22), and which has the value  $F_0 = 0.13n^{-4}$ . Still higher fields will cause the energy level to emerge into the continuous spectrum for the state  $n_2 = n$  because in this case the electron orbit is directed opposite to the field. The field intensity in this case is given by  $F_0 = 0.38n^{-4}$ . Fig. 3 shows the field intensity at which the discrete level disappears, as well as the electron energy for this case, as a function of the parabolic quantum numbers. The comparison is made for the case when the component of the angular momentum of the electron along the field direction is  $m = 0$ , so that  $n_1 + n_2 \approx n$ .

Disintegration of a highly excited atom placed in an electric field actually occurs for  $F < F_0$ . For this reason, we will determine below the ionization frequency

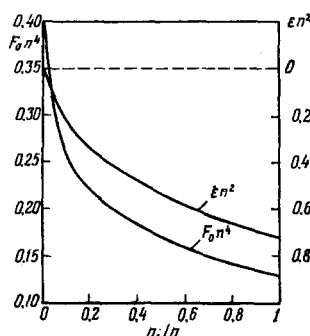


FIG. 3. The intensity of the electric field  $F_0$  at which the energy level of a highly excited electron emerges into the continuous spectrum and the electron energy  $\epsilon$  at this field intensity.  $n_1, n_2$ —parabolic quantum numbers of the electron; the azimuthal quantum number  $m = 0$ , so that  $n_1 + n_2 \approx n$ .

<sup>71</sup> Usually, this method is used to determine the effective quantum number, which can differ from the principal quantum number [see Eq. (4a)]. In order to simplify the notation, we do not make this distinction in our analysis.

TABLE VIII. Critical fields at which disintegration of a state with given  $n$  occurred in various experiments.

Excited atom	Method of producing atom	Range of values of the principal quantum number	V/cm	References
H	Charge exchange	9-22	6.5	9
H	"	9-16	6.8	29
He	"	9-17	5.8	29
H	"	9-28	6.0	30
H	"	19-28	6.5	31
H	Electron impact dissociation	15-19	6.3	41
N	Same	15-19	6.3	41
He, Ne, Ar, Kr,	Electron impact excitation	20-80	6.0	42
Xe	Laser excitation	26-37	3.1	80
Na	"	24-40	4.6	81
Xe	"	28-80	3.2	84
Rb	"	30-85	3.2	84
Cs	"	16-21, $l=m=0$	4.7	82
Na	"	16-19, $l=1, m=0$	3.7	82
		16-19, $l=1, m=1$	3.9	82
		15-19, $l=2, m=0$	3.6	82
		15-19, $l=2, m=1$	3.8	82
		15-19, $l=2, m=2$	4.3	82
Average value			4.9±1.3	

of the highly excited atom as a function of the electric field intensity in the parameter range  $n \gg 1, F_0 - F \ll F_0$ . We will limit ourselves to the exponential dependence that is determined by the penetrability of the barrier and is given by the formula

$$w \sim \exp \left( -2 \int_{z_1}^{z_2} |p| dz \right), \quad (23)$$

where  $p = \sqrt{2(U - \epsilon)}$ ;  $z_1$  and  $z_2$  are points at which the integrand vanishes:  $p(z_{1,2}) = 0$ . Using Eq. (16) and computing the integral using the assumptions made above, we obtain:

$$w \sim \exp \left( -2\pi \sqrt{2} n \frac{F_0 - F}{F_0} \right). \quad (24)$$

Taking into account only the exponential dependence on the electric field intensity makes sense when the exponent is sufficiently large. Since  $n \gg 1$ , this is in fact the case and in a part of the parameter space being considered we have  $F_0 - F \ll F_0$ .

According to Eq. (24), the ionization probability for the highly excited atom per unit time in an electric field decreases sharply with decreasing field, when the transition has a tunneling character (i.e.,  $F < F_0$ ). On the other hand, the electric field intensity at which the term of interest emerges into the continuous spectrum itself depends strongly on the quantum numbers of the state. For this reason, the picture of the disintegration of excited atomic states in an electric field turns out to be quite complicated. It is easy to establish experimentally the electric field intensity at which disintegration first occurs. Since this quantity does not depend strongly on the transit time of the highly excited atom in the electric field, it may be assumed in first approximation that disintegration first occurs at a field intensity for which the first level in the group of levels corresponding to the given state emerges into the continuous spectrum. The intensity of this field is described by the similarity relation  $F_c n^4 = \text{const.}$  and, in addition, if  $F_c n^4 = 0.13$ , then this quantity equals  $6.7 \cdot 10^8$  V/cm. Table VIII displays the experimental values of the quantity  $F_c n^4$  obtained under suitable experimental conditions.

## 5. COLLISIONS BETWEEN HIGHLY EXCITED ATOMS AND CHARGED PARTICLES

Collisions between highly excited atoms and charged particles lead to the most efficient transitions between the states of a highly excited atom. This is due to the long range character of the interactions between the incident particle and the weakly bound electron. For this reason, for fairly slow collisions, the cross section for the electron transition is comparable to the square of the size of the electron orbits, which equals<sup>16</sup>

$$\bar{r}^2 = \frac{n^3}{2} [5n^2 + 1 - 3l(l+1)]. \quad (25)$$

Let us examine the collision of an atom in a Rydberg state with an electron. Electron collisions are most effective for causing transitions between Rydberg states. This is due, on the one hand, to the small mass and correspondingly high electron speed. On the other hand, the long-range character of the Coulomb interaction between the incident particle and the weakly bound electron is important so that electron impact quenching of atomic Rydberg states is characterized by large cross sections of the order of the cross section of the excited atoms. Consequently, electron impact quenching of atomic Rydberg states becomes important in weakly ionized gases even with a very small degree of ionization of the gas.

The theoretical study of collisions between an electron and a highly excited atom at first proceeded along two directions. On the one hand, the theory depended on the methods of quantum mechanical perturbation theory, using the Born and the Born-Coulomb approximations and the method of sudden perturbations for describing collisions between electrons and highly excited atoms and, often, the dipole approximation for the interaction between an incident electron and a weakly bound electron, and so on (see Refs. 83-96). As subsequent studies have shown, perturbation theory can be used to compute the correct result for transitions to neighboring levels for sufficiently large collision velocities.

The other direction for the theory depended on the purely classical representation of the motion of a weakly bound electron, so that the collision was described as a collision between two classical electrons in a Coulomb field. This description was first used by Grizinski<sup>97</sup> but the specific realization of the classical concepts in his work does not withstand serious criticism. The classical approach to this problem was subsequently clearly formulated<sup>98-107</sup> and the problem was stated unambiguously. The electrons exchange energy as a result of the collision in a Coulomb field, and this uniquely determines the final state of the excited electron. The classical problem itself is a three-body problem because in the scattering process the Coulomb interactions between the electrons and the atomic core are important. For this reason, the result cannot be represented in analytic form and a more convenient method in this case is the Monte Carlo method, which provides a numerical solution to the problem. Analysis shows that the classical approaches are valid for transitions to the upper highly excited levels or into the

continuous spectrum.

A correct theory describing collisions of electrons with highly excited atoms must use a quasiclassical (rather than classical) concept of the weakly bound electron. Such an approach was formulated and developed in Refs. 106 and 108–110 and is presented in Ref. 121. The difficulties of this approach arise due to the need of taking into account transitions between many states, a problem which we encounter as soon as we abandon perturbation theory. However, the problem is simplified if we assume that the excited levels are equidistant. This is valid for large quantum numbers  $n \gg 1$  and results in the fact that the characteristics of the transitions depend only on the difference of the principal quantum numbers  $\Delta n$ , which significantly simplifies the problem. Such a quasiclassical approach allows determining the cross section for the transition for  $\Delta n \ll n$ . In this way, the quasiclassical approach provides a bridge between the results obtained with the use of normalized perturbation theory and valid for  $\Delta n = 0, 1$ , and the results of the classical approaches corresponding to the region  $\Delta n \gg 1$ .

Experimental studies of the transitions between highly excited atomic states as a result of collisions with electrons are at the present time very limited. However, since experimental techniques have recently been perfected for studying atoms in Rydberg states, there is no doubt that experimental studies will soon proceed along these lines in full force. The quenching of highly excited atomic states due to collisions with fast electrons is studied in Refs. 41 and 42. A beam of electrons with energies in the 100 eV range produced the highly excited states in inert gas atoms and also caused their partial quenching. The dependence on the beam intensity of the rate at which atoms in a given state are formed allows establishing the quenching cross section, which in the range of parameters being considered is well approximated by the function

$$\sigma_{\text{quench}} = \frac{6.6n^4}{E} \ln(4En^2). \quad (26)$$

It is of interest to compare this expression with the Born cross section, which has the form<sup>17</sup>

$$\sigma_{\text{quench}} = \frac{5\pi n^4}{3E} \ln(cEn^2) = \frac{5.2n^4}{E} \ln(cEn^2), \quad (27)$$

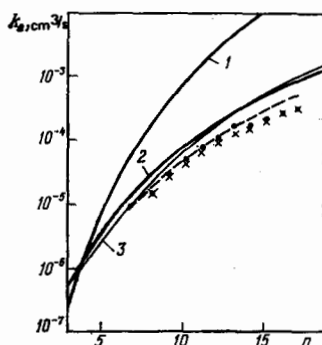


FIG. 4. Electron collisional quenching rate constants for the stage  $\text{He}(n^3P)$  at an electron temperature of 400 K. ●—experiment<sup>52</sup>; theory: 1—Ref. 97; 2—Refs. 101, 107; 3—Ref. 96; ×—Eq. (28).

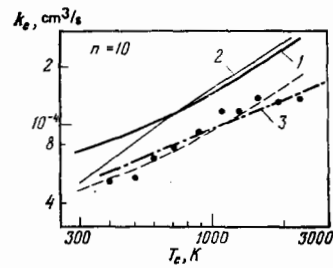


FIG. 5. Electron collisional quenching rate constants for  $\text{He}(10^3P)$  as a function of electron temperature. ●—experiment<sup>52</sup>; theory: 1—Refs. 101, 107, 2—Ref. 96, 3—Eq. (28).

where the numerical factor  $c$  is of the order of unity. In obtaining this expression, we assumed that the orbital angular momentum of the electron is relatively small ( $l \ll n$ ). This corresponds to the experimental conditions and yields  $\bar{d}_x^2 = (5/6)n^4$  ( $d_x$  is the dipole moment operator of the highly excited atom).

The quenching of highly excited atomic states due to collisions with slow electrons was studied in Refs. 51–53. In this experiment, one of the transitions in  $\text{He}(2^3S \rightarrow n^3P)$ , where  $n = 8–17$ , was excited with the help of a tunable laser. Helium was first excited with an electric discharge and contained a fairly large number of atoms in the metastable  $2^3S$  state. The  $n^3P$  state was observed. The post-discharge weakly ionized helium plasma contains slow electrons and collisions involving these electrons caused the transitions between the highly excited atomic states. Figs. 4–6 show the results of these measurements with a constant quenching rate for the corresponding states.

In order to interpret the results theoretically, we will use simple considerations that include the physics of the process and that allow obtaining the transition rate constants as a function of the parameters of the problem. If the incident electron is assumed to move along a trajectory, then it is easy to show that perturbation theory breaks down for not very large collision speeds and for impact parameters that are small in comparison with the dimensions of the atom. Consequently, for these impact parameters, the quenching probability of the excited state equals unity. For impact parameters that are large in comparison with the dimensions of the excited atom, the quenching probability is small because the interaction between the elec-

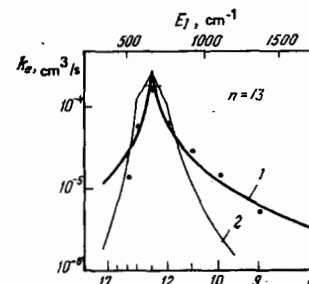


FIG. 6. Electron collisional quenching rate constants for  $\text{He}(13^3P)$  with a transition to other states at an electron temperature of 400 K. Experiment: 1, ●—Ref. 52; theory: 2—Ref. 96.

tron and the atom is small. This determines the order of magnitude of the maximum quenching cross section of the highly excited atom by electron impact as the square of the atomic dimensions, as determined by Eq. (25). For this reason, for  $n \gg l$ , the quenching cross section varies with increasing excitation of the atom as  $n^4$ . Taking this into account together with the experimental data, we represent the quenching rate constant in the form

$$k_{\text{quench}} = \sigma_0 \sqrt{\frac{2T_e}{m}} n^4, \quad (28)$$

where the quantity  $\sigma_0 \sim 10^{-16} \text{ cm}^2$ . From the condition that Eq. (28) should describe the experiment well, we choose  $\sigma_0 = 3.6 \cdot 10^{-16} \text{ cm}^2$ . Fig. 5 shows the results of a comparison with this formula.

We note that the semi-empirical formula (28) is valid in the range where  $T_e \sim 1/n^2$ . As the electron energy increases, for  $T_e \gg 1/n^2$ , the quenching rate constant must decrease in accordance with the results of the Born approximation. This assertion contradicts the results obtained in Ref. 53, where the data of Fig. 5 are extended into the range of higher electron temperatures up to  $T_e \sim 8,000 \text{ K}$ . According to the results of this experiment, in the temperature range considered  $T_e n^2 \gg 1$ , the quenching rate constant for the state with principal quantum number  $n = 10$  is approximated by a function close to  $k_{\text{quench}} \sim T_e$ .

The ionization process involving the collision of an electron with a highly excited atom is of particular interest. From general considerations, it follows that in this case the classical description of electron motion is valid. Indeed, with the usual statement of the problem, we can assume that if as a result of the collision the energy of the incident electron decreases by an amount exceeding the ionization potential of the atom, then ionization will occur. The ionization potential of the atom is given by  $1/2n^2$ , while the distance between neighboring electron levels is given by  $1/n^3$ , so that for  $n \gg 1$ , the discreteness of the energy of the initial state of the electron is not important for examining the process. Thus, the classical description of the ionization of a highly excited atom by an electron is correct.

The classical approach to studying the electron impact

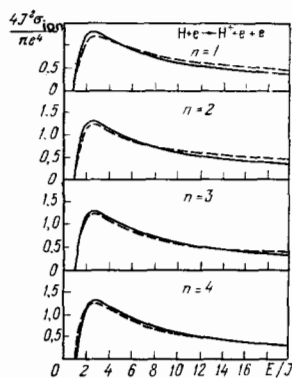


FIG. 7. Electron impact ionization cross section for a hydrogen atom in various excited states.<sup>117</sup> Solid line—classical theory; dashed line—Born approximation.

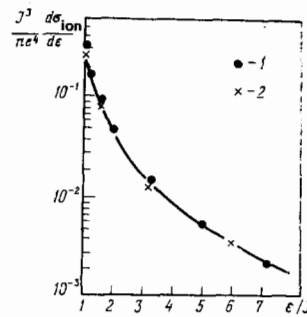


FIG. 8. Energy spectrum for electrons produced by electron impact ionization of a hydrogen atom for incident electron energy 9 times greater than the ionization potential of the atom.<sup>117</sup> Solid line—classical theory; Born approximation: 1— $n = 1$ ; 2— $n = 3$ .

ionization of an atom was the basic approach used in Refs. 111–113 at the early stages in studying this problem. The interest in the classical theory of electron impact ionization of an atom decreased after Bethe<sup>14</sup> obtained a quantum mechanical formula for the cross section in the Born approximation. For high incident electron energy  $E$ , this formula yielded the function  $\ln E/E$  for the ionization cross section, while any classical approach, including the subsequent classical calculations of the cross section for this process using the Monte Carlo method (for example, Ref. 98) yielded the dependence  $1/E$  for high electron energies. This discrepancy was resolved in Refs. 115–118, wherein it was shown that the disagreement between the Born and the classical approximations disappears as the excitation level of the valence electron increases. According to the analysis performed in the references indicated, in the limit  $n \rightarrow \infty$  the Born approximation, as well as the classical approach, which neglects the interaction of the electrons with the atomic core at the instant the electrons are scattered, give close results. As an illustration of this fact, Figs. 7 and 8 show the cross sections for electron impact ionization of the hydrogen atom, calculated in the classical and Born approximations, as well as the spectra of the free electrons produced.<sup>117</sup>

Among the processes involved in the collision of an ion with a highly excited atom, the most interesting process is charge exchange between the ion and the atom. The cross section for this process is comparable to the dimensions of the highly excited atom. Fig. 9 illustrates a section of the potential surface within which the electron moves in the case of a slow approach of an ion

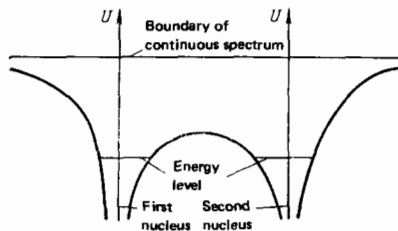


FIG. 9. Profile of the potential in which the electron moves during charge exchange between an ion and a highly excited atom.

to an excited atom. For some distance  $R_0$  between the nuclei, the potential barrier that separates the active regions of the ions disappears so that it is possible for an electron to move from one ion to the other along a classically accessible path. Thus, for slow collisions, the cross section for resonant charge exchange is given by<sup>119, 120</sup>

$$\sigma = \frac{\pi R_0^2}{2} \quad (29)$$

The factor  $1/2$  takes into account the fact that for slow collisions the electron has time to undergo many transitions between the potential wells so that the probability that the electron is located in the second well equals  $1/2$ .

The distance  $R_0$  at which the barrier between the potential wells disappears is of the order of the dimensions of the highly excited atom  $R_0 \sim n^2$ . This quantity depends on the quantum numbers of the electron. For a given principal quantum number  $n$ , the largest value of  $R_0$  corresponds to the state for which the electron orbit is most strongly elongated along the axis connecting the nuclei ( $n_z=0, n_y=2n$ ). For this state,  $R_0$  and the electronic energy  $\varepsilon$  are equal to

$$R_0 = \frac{\pi^2 n^2}{2}, \quad \varepsilon = -\frac{8}{\pi^2 n^2} \quad (30)$$

This result is confirmed by perturbation theory<sup>122</sup> (see also Refs. 123–125). It is also important that  $R_0$  depends not only on  $n$  but also on other quantum numbers. However, if it is assumed that the main dependence is related to the principal quantum number, an assumption which according to Eq. (30) is well satisfied, then we can obtain a universal formula for the charge exchange cross section. This assumes that if during a collision between an ion and a highly excited atom the position of the electron changes significantly, while its energy changes very little (the electron weakly exchanges energy with the nuclei during the collision), then, as before, in finding the cross section for resonant charge exchange, we can use only the ionization potential  $J$  to describe the state of the electron. Since the cross section for resonant charge exchange is related to the transition of a classical electron, then using dimensional analysis (we have the parameters  $e^2, m, J$ , and  $v$ , the collision velocity), the cross section for resonant charge exchange can be represented in the form

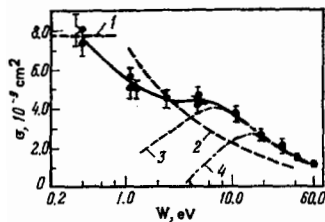


FIG. 10. Cross section for the loss of its electron by a highly excited hydrogen atom with  $44 \leq n \leq 50$  in a collision with a proton as a function of the collision energy. ●—experiment,<sup>32</sup> theory for  $n=47$ : resonance charge exchange: 1—Eqs. (29), (30), 2—Eqs. (31), (32); ionization: 3—Born approximation,<sup>83</sup> 4—classical calculation.<sup>98</sup>

$$\sigma = \frac{\pi R_0^2}{2} f\left(\frac{v}{\sqrt{2J/m}}\right), \quad (31)$$

where  $f(x)$  is a universal function for the process and  $f(0)=1$ .

For high collision speeds, the charge exchange cross section is inversely proportional to the collision speed. Indeed, the probability of a transition for an arbitrary impact parameter in this case is small and is proportional to the time over which an electron can make a transition from one core to the other, i.e., it is inversely proportional to the collision speed. The charge exchange cross section computed in Refs. 126 and 127 over the range of speeds considered yields the following universal function in Eq. (31):

$$f(x) = \frac{0.4}{x}, \quad x \gg 1. \quad (32)$$

Fig. 10 shows a comparison of Eqs. (30) and (32) for the resonant charge exchange cross section of a highly excited atom with an experiment<sup>32</sup> in which the cross section for a highly excited atom to lose an electron during a collision with an ion was measured. For low collision speeds, this cross section coincides with the charge exchange cross section, while for high speeds it coincides with the cross section for ionization of the highly excited atom.

Let us evaluate the role of the sub-barrier transitions during resonant charge exchange between an ion and a highly excited atom. The overall method for taking into account sub-barrier transitions is presented in Refs. 128 and 129. Our aim is to take into account the contribution of sub-barrier transitions for low collision speeds. For this purpose, we will estimate the exponential dependence for the potential describing the exchange interaction between the ion and the atom  $\Delta(R)$ , which is determined by the function<sup>127, 130</sup>  $\Delta(R) \sim \psi^2(R/r)$ , where  $\psi(r)$  is the wave function of the electron at a distance  $r$  from the nucleus. In correspondence with this formula, the exponential dependence for the exchange interaction potential has the form

$$\Delta(R) \sim \exp\left[-2 \int_{z_0}^{R/2} \sqrt{2(U-\varepsilon)} dz\right]. \quad (33)$$

Here,  $z$  is the coordinate along the axis joining the nuclei,  $U$  is the potential of the interaction between the electron and the cores, when the electron is located on the axis,  $\varepsilon$  is the energy of the electron, and  $z_0$  is the turning point, i.e.,  $U(z_0)=0$ .

We will assume that  $\Delta R = R - R_0 \ll R_0$ . In this case, we have

$$U - \varepsilon = -\frac{1}{z} - \frac{1}{R-z} + \frac{1}{R} + \frac{1}{2n^2} = \frac{3\Delta R}{R^2} - \frac{16\left(\frac{R}{2} - z\right)^2}{R^2},$$

which gives the following exponential dependence for the exchange interaction potential:

$$\Delta(R) = A \exp\left[-\frac{3\pi(R-R_0)}{4(2R_0)}\right] = A \exp\left[-\frac{3(R-R_0)}{4n}\right], \quad (34)$$

where  $A$  is the pre-exponential multiplier and it is assumed that  $R_0 = \pi^2 n^2 / 2$ . We will now compute the contribution to the charge exchange cross section for low speeds due to the sub-barrier transitions, using the following formula for the charge exchange cross sec-

tion<sup>127</sup>:

$$\sigma_{ex} = \frac{\pi \rho_0^2}{2}, \text{ where } \int \Delta(R) dt |_{\rho=\rho_0} = 0.28, \quad (35)$$

where  $\rho_0$  is the impact parameter of the collision, for which the last relation is satisfied, and, in addition  $\rho_0 > R_0$ . Computing this integral, we find the relation for  $\rho_0$ :

$$\frac{v}{v_0} = \exp \left[ -\frac{3}{4n} (\rho_0 - R_0) \right],$$

where the parameter  $v_0$  does not depend on the collision speed  $v$ . Solving for  $\rho_0$  and substituting the result into the charge exchange cross section, we find, taking into account the fact that  $\rho_0 - R_0 \ll R_0$ , that

$$\sigma_{ex} = \frac{\pi \rho_0^2}{2} = \frac{\pi R_0^2}{2} + \Delta\sigma, \text{ where } \Delta\sigma = \pi R_0 (\rho_0 - R_0) = \frac{4\pi n}{3} \ln \frac{v_0}{v}. \quad (36)$$

From this we obtain:

$$\frac{\Delta\sigma}{\sigma_{ex}} = \frac{16}{3\pi^2 n} \ln \frac{v_0}{v}. \quad (37)$$

Here,  $\Delta\sigma$  represents that part of the charge exchange cross section that is determined by the sub-barrier transitions, i.e., by impact parameters  $\rho > R_0$ . It is evident that for a highly excited atom  $n \gg 1$  and this part of the cross section is relatively small, i.e., sub-barrier transitions make a small contribution to the cross section for charge exchange between a highly excited atom and an ion.

## 6. IONIZATION OF A HIGHLY EXCITED ATOM AS A RESULT OF A COLLISION WITH ATOMIC PARTICLES

The process under consideration proceeds as follows:



and involves the transition of an electron into the continuous spectrum. Since the electron in the atom is in a highly excited state, the analysis of this process is greatly simplified for the following reasons. First of all, the size of the region in which the electron interacts with the incident atomic particle is much smaller than the size of the excited atom. Second, the motion of the electron in the atom can be described by classical laws because the change in the energy of the electron for the transition of interest, which varies as  $1/n^2$  ( $n$  is the principal quantum number), greatly exceeds the difference between the energies of neighboring levels, which equals  $1/n^3$ . Thus, the discreteness of the energy levels of the electron is not important for the given process.

The properties of the process noted above permit separating the interaction of the electron with its own core and the collision of the electron with the incident atomic particle. These properties of the process make it possible to describe it using the same model that we used to study the process of electron impact ionization of a highly excited atom. In particular, we will examine the process (38) as the result of the scattering of a classical electron by an incident atomic particle. If during such a collision a quantity of energy exceeding the binding energy of the electron is transferred to the electron, then ionization occurs.

Using the given model, we will obtain an expression

for the ionization cross section, which we will use for analyzing particular cases. The ionization probability under the conditions of the model equals  $N \langle |\mathbf{v} - \mathbf{v}_a| \int d\sigma \rangle$  per unit time, where  $N$  is the density of incident atoms,  $\mathbf{v}$  is the velocity of the electron,  $\mathbf{v}_a$  is the relative velocity of the nuclei,  $d\sigma$  is the cross section for scattering of the electron by the atom, the integral with respect to  $d\sigma$  corresponds to those scattering angles for which the energy transferred from the atom to the electron exceeds the binding energy of the electron in the atom  $J$ , and the angular brackets denote an average with respect to the electron velocity in the atom. Dividing this quantity by the flux of incident atoms  $Nv_a$ , we obtain an expression for the ionization cross section<sup>131-133</sup>

$$\sigma_1 = \left\langle \frac{|\mathbf{v} - \mathbf{v}_a|}{v_a} \int_{\Delta E \geq J} d\sigma \right\rangle. \quad (39)$$

In particular, in the limit  $v_a \gg 2/n$ , this formula yields<sup>131-134</sup>

$$\sigma_1 = \sigma_e(v_a), \quad (40)$$

where  $\sigma_e$  is the cross section for elastic scattering of the electron by the atom.

Fig. 11 shows a comparison of the right and left sides of Eq. (40).<sup>135, 136</sup> The ionization cross section of a highly excited deuterium atom colliding with a nitrogen molecule<sup>135, 136</sup> is compared with the cross section for elastic scattering of an electron by the molecule.<sup>137, 138</sup> The collision velocity varies over a fairly large range so that in this region the cross section for elastic scattering of the electron by the molecule undergoes a change. As can be seen from Fig. 11, in the example being considered, not only are the absolute cross sections that make up the left and right part of Eq. (40) nearly equal, but there is a tendency for the two cross sections to have the same dependence on the collision velocity.

The ionization cross section for highly excited atoms colliding with neutral particles becomes large if there is a resonance in the low-energy elastic scattering of an electron by this particle. This occurs during collisions of highly excited atoms with complex molecules that contain halogens. In this case, the rate constants of the process are obtained from Eq. (39)<sup>132, 133, 135</sup>:

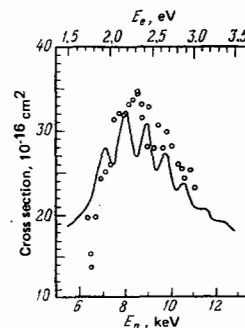


FIG. 11. Ionization cross section for a highly excited deuterium atom ( $35 \leq n \leq 50$ ) colliding with a nitrogen molecule<sup>135, 136</sup> (circles) compared with the cross section for elastic scattering of an electron by a nitrogen molecule (solid line<sup>137, 138</sup>).

$$k_i = v_a \sigma_i = \left\langle |v - v_a| \int_{\Delta R} d\sigma \right\rangle. \quad (41)$$

Here, the average is taken as previously with respect to the velocities of the weakly bound electron and the formula is valid if the cross section for scattering of the electron by the molecule is small in comparison with the diameter of the highly excited atom.

The process being considered here was studied experimentally in Refs. 140–142. In this work, the rate constant was measured for ionization of the states of xenon  $Xe(nf)$  with  $n=25-41$  as a result of a collision at thermal energies with a number of complex molecules such as  $SF_6$ ,  $CCl_4$ ,  $CCl_3F$ ,  $C_7F_{14}$ ,  $C_6F_6$ ,  $CH_3I$ , and  $CH_3Br$ . The rate constant for the process being studied in several cases increases with increasing principal quantum number  $n$  ( $CCl_4$ ,  $CCl_3F$ ,  $CH_3I$ ); for the  $SF_6$  molecule, the rate constant for the process of interest does not depend on the principal quantum number and amounts to<sup>141</sup>  $4 \cdot 10^{-7} \text{ cm}^3/\text{s}$ ; for  $C_7F_{14}$ , the cross section of the process decreases with increasing principal quantum number.

Fig. 12 shows a comparison of the ionization rate constant for a highly excited xenon atom colliding with a  $CCl_4$  molecule and the rate constant for dissociative attachment of the electron by this molecule.<sup>143–145</sup> As can be seen, there is some correspondence between these properties. The ionization cross section varies with increasing principal quantum number approximately as  $\sigma_i \sim n$ , which corresponds to a dependence  $\sigma_e \sim 1/v$  for the cross section for scattering of the electron by the molecule as a function of the electron speed  $v$ . We note that in the cases being examined the large magnitude of the ionization cross section is related to the resonance nature of the scattering of the electron by the molecule, which is accompanied by ionization of the molecule. In this case, Eq. (41) usually includes the cross section for capture of the electron by the molecule regardless of the final channel for the process, which for complex molecules usually involves dissociative attachment.

The mechanism for ionization of the highly excited atom colliding with a neutral particle as examined above depends on the fact that the electron acquires enough energy from this particle to become a free electron. In the case of a collision with a molecule, this energy can be obtained from the internal degrees of freedom of the molecule, such as the excitation energy of the rotational states. Thus, the ionization cross section in the given case, according to Eq. (39), equals<sup>131–133, 146–152</sup>:

$$\sigma_i = \frac{\langle |v - v_a| \sigma_{rot} \rangle}{v_a}, \quad (42)$$

where  $\sigma_{rot}$  is the cross section for quenching the rotational excitation of the molecule by electron impact and, in addition, we assume that the ionization potential of

<sup>8)</sup>The collision cross section equals  $\sigma_i = 1.3 \cdot 10^{-11} \text{ cm}^2$ . This corresponds to the condition for the applicability of the impulse approximation  $n \gg n_0$ , where  $n_0$  satisfies the relation  $\sigma_i = (5/2)\pi n_0^4$  and, in this case,  $n_0 = 16$ . In the case of collisions with other molecules, the ionization cross section also turns out to be of the order of  $10^{-11} \text{ cm}^2$ .

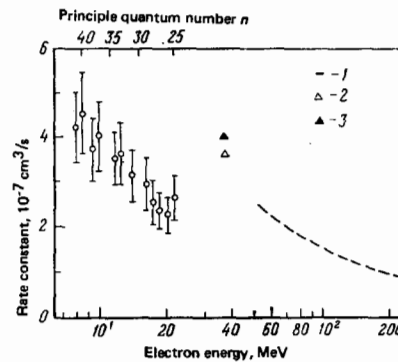


FIG. 12. Rate constant for ionization of  $Xe(nf)$  colliding with a  $CCl_4$  molecule (open circles)<sup>141</sup> and the coefficient for dissociative attachment of an electron by the  $CCl_4$  molecule (1—Ref. 143, 2—Ref. 144, 3—Ref. 145).

the highly excited state of the atom is less than the change in the rotational energy of the molecule.

In this case, the cross section for ionization of the highly excited atom is determined by the nature of the interaction between the slow electron and the molecule. For simplicity, in what follows we will consider low collision velocities

$$v_a n \ll 1 \quad (43a)$$

and at the same time highly excited states, for which the characteristic change in the rotational energy  $\Delta E_{rot}$  is large in comparison with the ionization potential of the atom  $J$ :

$$\Delta E_{rot} \gg J. \quad (43b)$$

Since the change in the rotational energy is  $\Delta E_{rot} \sim B_j$ , where  $B$  is the rotational constant of the molecule,  $j$  is the angular momentum, and for a gas temperature  $T$  the most probable value of the angular momentum is  $j \sim \sqrt{T/B}$  ( $T \gg B$ ), the condition (43b) assumes the form<sup>9)</sup>

$$J \ll \sqrt{BT}. \quad (44)$$

Taking into account the conditions (43), Eq. (42) for the ionization cross section of a highly excited atom colliding with the molecule has the form:

$$\sigma_i = \frac{\langle v \sigma_{rot} \rangle}{v_a}, \quad (45)$$

where  $\sigma_{rot}$  is the cross section for electron impact quenching of rotational excitation of the molecule. Table IX summarizes the formulas<sup>131–133</sup> for the ionization cross section of a highly excited atom colliding with a rotationally excited molecule. They are based on the Born expression for the cross section for the change in the rotational state of the molecule during the collision of an electron with a dipole<sup>153, 154</sup> and a quadrupole<sup>155</sup> molecule, which are valid in the limit of low electron collision velocities. These formulas correspond to the conditions (43) being satisfied, and av-

<sup>9)</sup>Since the rotational constant of the molecule is of the order of  $1/\mu$  in atomic units, where  $\mu$  is the mass of the nuclei, and  $T \sim \mu v_a^2$ , the condition (44) can be represented in atomic units as

$$v_a \gg \frac{1}{n^2}. \quad (44a)$$

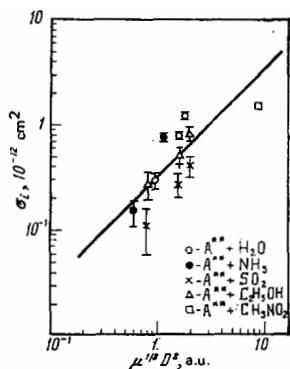


FIG. 13. Ionization cross section for a highly excited atom colliding with a dipole molecule (experiment)<sup>156</sup> as a function of the parameter  $D^2\sqrt{\mu}$  (Ref. 148). The straight line corresponds to linear dependence of the cross section on the parameter indicated.

eraging with respect to the rotational states of the molecule is performed assuming that  $j \gg 1$ .<sup>10)</sup>

In the case of a collision with a dipole molecule, according to Table IX the dependence of the ionization cross section for a highly excited atom on the characteristics of the dipole molecule is expressed in terms of the parameter  $D^2\mu^{1/2}/B^{1/2}$ , where  $D$  is the dipole moment of the electron,  $\mu$  is the reduced mass of the nuclei, and  $B$  is the rotational constant of the molecule.<sup>11)</sup>

In order to demonstrate this relationship, Fig. 13 shows the ionization cross sections, taken from Ref. 148, for a number of highly excited atoms colliding with dipole molecules, as a function of the parameter  $D^2\sqrt{\mu}$ , plotted along the abscissa axis. The experimental data from Ref. 156 were used. Other measurements of the cross sections for the given process are described in Refs. 157–168 and 181. Figs. 14 and 15 show the measurements of the ionization rate constants for highly excited atoms colliding with water and ammonium molecules, respectively, taken from Ref. 160. These rate constants are comparable with the computational results obtained using the impulse approximation,<sup>140</sup> as well as the asymptotic expression for the ionization rate constant, which is, valid when condition (43b) is satisfied and, according to the expressions in Table IX, has the form

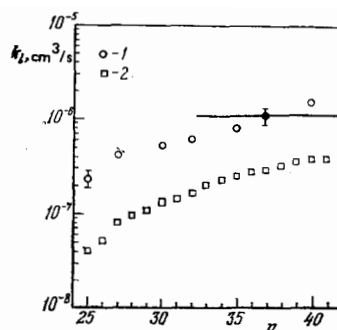


FIG. 14. Rate constant for ionization of a  $Xe(nf)$  atom colliding with a water molecule. 1—experiment,<sup>160</sup>; 2—impulse approximation,<sup>152</sup> solid line—asymptotic limit for  $n \rightarrow \infty$  according to Eq. (46).

$$k_i = \frac{5.1D^2}{(BT)^{1/4}}. \quad (46)$$

We note that the boundary for violation of the condition (43b)  $\Delta E_{rot} = J$  for rotational angular momentum of the molecule  $j = \sqrt{T/B}$  corresponds to  $n = 32$  for water molecules and  $n = 35$  for ammonium molecules.

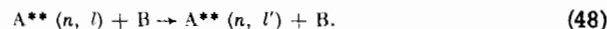
## 7. QUENCHING OF ATOMIC RYDBERG STATES BY COLLISIONS WITH ATOMS AND MOLECULES

The disintegration processes for the atomic Rydberg states being considered as a result of collisions with atoms and molecules can be conventionally separated into two types. The first type includes transitions to states with different quantum numbers:



For such collisions, the ionization potential of the electron changes so that these reactions play a role in processes such as stepwise ionization of atoms in highly excited states by collisions with atoms and molecules, as well as in three-body recombination of the electron and a molecular ion, when the third body is an atom or molecule.

The other type of process studied involves the change in the orbital angular momentum of the highly excited atoms



Processes of this type can be easily studied experi-

<sup>10)</sup> In order to estimate the range of applicability of the formulas, let us consider the conditions for applicability to nitrogen molecules ( $B = 2 \text{ cm}^{-1}$ ) and  $T = 300 \text{ K}$ . In this case, (43a) has the form  $n \ll 4 \cdot 10^3$ , while the condition (43b) with  $j_0 = \sqrt{T/B}$  ( $j_0 \approx 10$ ) gives  $n \gg 40$ .

<sup>11)</sup> The formulas used for the cross sections for an elastic collision of an electron with a molecule correspond to linear molecules (see Table IX). Latimer's work<sup>151</sup> presents calculations of ionization cross sections of highly excited atoms for collisions with symmetric and linear molecules  $\text{NH}_3$ ,  $\text{H}_2\text{S}$ ,  $\text{SO}_2$ , and  $\text{HCl}$ , using for the symmetric molecules the cross sections for inelastic collisions of electrons with these molecules, which were taken from Ref. 154. We note that in the case of linear and symmetric molecules there is no essential difference in the cross section being considered.

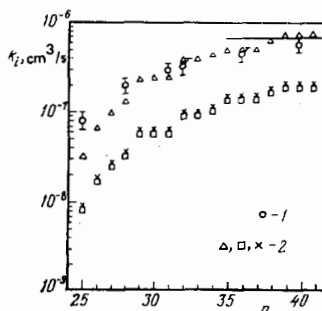


FIG. 15. Rate constant for ionization of a highly excited  $Xe(nf)$  atom colliding with an ammonia molecule. 1—experiment<sup>160</sup>; 2—different versions of the impulse approximation<sup>152</sup>; solid line—asymptotic limit for  $n \rightarrow \infty$  [Eq. (46)].

TABLE IX. Summary of data on the ionization cross sections for highly excited atoms colliding with a rotationally excited linear molecules.

Type of molecule	Electron impact quenching of a molecular rotational level		Ionization cross section for a highly excited atom satisfying conditions (43)	
	Selection rule for the rotational transition	Cross section for the rotational transition in the Born approximation	For a given value of the angular momentum of the molecule	Average with respect to the distribution of molecules in rotational levels and with respect to translational motion
Dipole	$j \rightarrow j-1$	$\frac{4\pi D^2}{3E} \frac{j}{2j+1} \times \ln \frac{\sqrt{1 + \frac{2Bj}{E}} + 1}{\sqrt{1 + \frac{2Bj}{E}} - 1}$	$\frac{8\pi D^2}{3(2j+1)v_a} \sqrt{\frac{j}{B}}$	$\frac{3.22 D^2 \mu^{1/2}}{B^{1/4} T^{3/4}}$
Quadrupole	$j \rightarrow j-2$	$\frac{8\pi Q^2}{15} \frac{j(j-1)}{(2j+1)(2j-1)} \times \sqrt{1 + \frac{2B(2j+1)}{E}}$	$\frac{16\pi Q^2}{15v_a} \times \frac{j(j-1)\sqrt{B}}{(2j+1)\sqrt{2j-1}}$	$\frac{0.74 Q^2 \mu^{1/4} B^{1/4}}{T^{1/4}}$

*D* is the dipole moment of the molecule, *Q* is the quadrupole moment of the molecule, *E* is the energy of the incident electron, *j* is the angular momentum of the molecule before the collision, *B* is the rotational energy of the molecule, *v<sub>a</sub>* is the relative velocity of the colliding nuclei, *T* is the temperature of the gas in which the process occurs, and *μ* is the reduced mass of the nuclei.

mentally using a simple technique. Highly excited atoms in a state with particular quantum numbers are created in the usual manner; the last step in the excitation is performed with a tunable laser with the help of which highly excited states are selectively populated. Then, the quenching of the fluorescence arising from the highly excited states being examined is measured as a function of time. The quenching cross section for the Rydberg state of interest as a result of collisions with atoms or molecules of the buffer gas is determined as a function of the buffer gas pressure.

Table X summarizes the results of experimental studies of the quenching of highly excited atomic states as a result of slow collisions. The quenching of these states is related to transitions with a small change in energy and as a result usually involve the process (48). We note that since the study of the fluorescence of highly excited atoms becomes greatly complicated with increasing principal quantum number of the state (see Sec. 4), the measurements cited correspond to quantum numbers *n* that are not very large.

The theoretical study of the process (47) begins with the work of Pitaevskii,<sup>183</sup> in which the three-body recombination of an electron and ion involving atoms was examined. In this process, for low electron tempera-

TABLE X. Experimental investigations of collisional quenching processes for Rydberg states.

Atom (excited state)	Range of values of the principal quantum number	Collision partner	References
Na ( <i>n</i> <sup>2</sup> D)	8-15	He, Ne, Ar	169-171
Na ( <i>n</i> <sup>2</sup> S)	6-11	He, Ar, Xe	172, 173
He ( <i>n</i> <sup>2</sup> P)	8-17	<sup>4</sup> He, <sup>3</sup> He	58
He ( <i>n</i> <sup>1</sup> S, <i>n</i> <sup>3</sup> S)	2-14	He, Ne, Ar	174
Rb ( <i>n</i> <sup>2</sup> P)	12-22	He, Ne, Ar, Rb	175
Rb ( <i>n</i> <sup>2</sup> S)	12-18	Rb	176
Rb ( <i>n</i> <sup>2</sup> S)	12-18	He	177
Rb ( <i>n</i> <sup>2</sup> D)	9-15	He	177
Rb ( <i>n</i> <sup>2</sup> F)	9-21	He, Ar, Xe, Rb	178
Cs ( <i>n</i> <sup>2</sup> S)	9-14	Cs	179
Cs ( <i>n</i> <sup>2</sup> D)	8-14	Cs	179
Cs ( <i>n</i> <sup>2</sup> S, <i>n</i> <sup>2</sup> D)	9-15	Cs	180
Xe ( <i>n</i> <sup>2</sup> J)	22-39	NH <sub>3</sub>	164

tures, an atom in a highly excited state is first formed, and then, as a result of collisions with buffer gas atoms, migration occurs along the levels of the excited atom. In Pitaevskii's work,<sup>183</sup> the diffusion coefficient along excited states, which determines the recombination coefficient of the electron and ion, was determined. In order to find this quantity, a model for transitions between highly excited states was introduced. This model is based on elastic scattering of the weakly bound electron by the atom. As a result, the rate of migration along the levels is expressed in terms of the cross section for elastic scattering of a free electron by the atom and the density of states of the weakly bound electron.

In estimating the cross section for inelastic scattering of the highly excited atom by an atom within the framework of the model examined, we note that the characteristic change in the energy of the electron as a result of elastic scattering by the atom is  $\Delta E \sim v_e v_a$ , where the electron velocity is  $v_e \sim 1/n$ . Since this energy greatly exceeds the difference in the energies of neighboring levels  $1/n^3$ , but is less than the binding energy of the electron in the atom  $1/n^2$ , we have

$$\frac{1}{n^2} \ll v_e \ll \frac{1}{n}. \quad (49)$$

We can determine the cross section for inelastic collisions of atoms in the case being examined according to Eq. (39), using in this formula the change in the electron energy corresponding to an inelastic transition. Under the conditions (49), Eq. (39) gives

$$\sigma_i \sim \frac{1}{v_a n} \sigma_e, \quad (50)$$

where  $\sigma_e$  is the cross section for elastic scattering of the electron by the atom. It is evident that the maximum cross section for an inelastic collision is of the order of  $n\sigma_e$ , i.e., it increases with increasing excitation.

We note that for the transitions being examined the Massey parameter equals

$$\frac{\Delta E a}{v_n} \sim n, \quad (51)$$

because the change in energy for an inelastic transition is  $\Delta E \sim (1/n)v_a$ , while the distance at which the parameters of the interacting particles change is  $a \sim n^2$ . According to the theory of atomic collisions,<sup>182</sup> the probability of a transition between two states involving a large Massey parameter  $\zeta \gg 1$  is adiabatically small ( $\sim e^{-\zeta}$ ). This discrepancy in the model used to describe the collision involving a highly excited atom is eliminated after taking into account the large number of states in the system. In each collision many states take part in the transition and the transition being examined is a result of the totality of transitions between a large number of closely spaced levels for which the Massey parameter is small. All these transitions occur during a single collision.

The free-electron model introduced by Pitaevskii for inelastic collisions between a highly excited atom and another atom was further developed by Bates and Khare<sup>184</sup> for use with the same problem, three-body recombination of electrons and ions involving atoms. This

work demonstrated the important role of the discreteness of the excited levels of the atom, which is manifested even for low numerical values of the ratio of the difference in the energies of neighboring levels to the characteristic change in the energy in the transitions. Further development of the ideas formulated in these studies led Flannery<sup>185, 186</sup> to construct a semi-classical theory of transitions between highly excited atomic states as a result of collisions. On the foundation of this work, Matsuzawa<sup>187-195</sup> formulated and developed the impulse approximation.<sup>12)</sup>

Numerous theoretical studies of the process (48) for a transition to a state with nearly equal energy<sup>197-204</sup> were based on the short-range character of the interaction between the weakly bound electron and the incident atom. Using this work,<sup>13)</sup> let us determine the properties of the cross section for the process (48). The operator for the short-range interaction between the weakly bound electron and an incident atom equals (in atomic units)

$$V = 2\pi L\delta(r - R),$$

where  $L$  is the scattering length for scattering of the electron by the atom,  $r$  is the position vector of the electron, and  $R$  is the position vector of the atomic nucleus. According to perturbation theory, the probability of a transition between the states  $i$  and  $k$  with nearly equal energies due to this interaction is given by

$$w_{i \rightarrow k} = \left| \int_{-\infty}^{+\infty} V_{ik} dt \right|^2 = 4\pi^2 L^2 \left| \int_{-\infty}^{+\infty} \psi_i^*(R) \psi_k(R) dt \right|^2, \quad (52)$$

where  $R$  is the position vector along the trajectory of the incident atom.

Equation (52) can be used to estimate the magnitude of the cross section for the process (48) and its dependence on the principal quantum number. Since the density of the weakly bound electron in the classically accessible region of motion is  $|\psi|^2 \sim 1/a^3 \sim 1/n^6$ , where  $a \sim n^2$  is the size of the highly excited atom and  $\int dt \sim a/v_a \sim n^2/v_a$ ,  $w_{i \rightarrow k} \sim L^2/v_a^2 n^8$  ( $v_a$  is the relative velocity of the nuclei). This gives the following result for the cross section of interest:

$$\sigma \sim a^2 w_{i \rightarrow k} \sim \frac{L^2}{v_a^2 n^4}, \quad \frac{L}{v_a} \ll n^4. \quad (53)$$

The condition for the applicability of this result stated on the right is  $w_{i \rightarrow k} \ll 1$ . The dependence shown in (53) was obtained in many of the cited studies<sup>195-202</sup> for particular transitions involving large values of  $n$ .

Let us analyze the result obtained. The quenching cross section for the Rydberg state of interest decreases sharply with increasing principal quantum number.

<sup>12)</sup>In the case of ionization of a highly excited atom the impulse and classical approximations for the electron require that identical conditions be satisfied.<sup>196</sup>

<sup>13)</sup>Although the polarization interaction between a weakly bound electron and an incident atom affects the magnitude of the quenching cross section for a Rydberg state, taking into account only the short-range part of the interaction potential elucidates the essence of the problem.

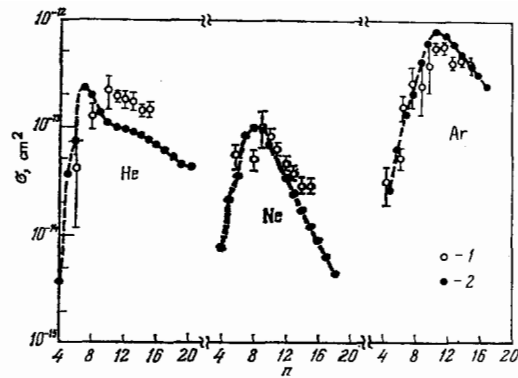


FIG. 16. Quenching cross section for a highly excited  $\text{Na}(n^2D)$  atom colliding with inert gas atoms. 1—experiment<sup>169, 170</sup>; 2—theory<sup>198</sup> for a transition to the state  $\text{Na}(n^2F)$ .

ber in the region where the quenching cross section is much less than the cross-sectional area of the atom. For small values of the principal quantum number, for which a condition opposite to (53) is satisfied, the quenching cross section for Rydberg states increases with increasing principal quantum number. In this case, the outer region of the atom provides the main contribution to the quenching cross section and the quenching cross section is comparable to the cross-sectional area of the excited atom. The cross section attains a maximum for values of the principal quantum number  $n_{\text{max}} \sim (L/v_a)^{1/4}$  and constitutes

$$\sigma_{\text{max}} \sim \frac{L}{v_a}. \quad (54)$$

For thermal collision velocities, this corresponds to  $n_{\text{max}} \sim 10$  and  $\sigma_{\text{max}} \sim 10^{-13} \text{ cm}^2$ .

Figures 16 and 17 show a comparison of theory with experiment for the cross sections for quenching of  $\text{Na}(n^2P)$  states by inert gas atoms. It is evident that the estimated order of magnitude is valid.

The analysis presented above involves transitions between states for which the orbital angular momentum is not too low. Let us estimate the magnitude of the Massey parameter for the transitions of interest. The difference in energies entering into this expression for the transition  $nl \rightarrow nl'$  equals  $\Delta E \sim (\delta_l - \delta_{l'})n^{-3}$ , where  $\delta_l$ ,

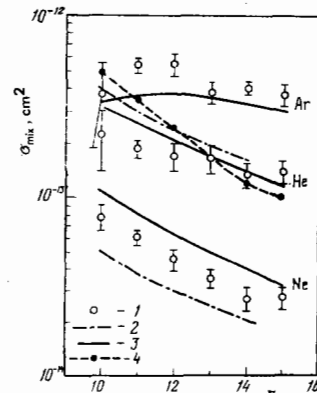


FIG. 17. Quenching cross section for a highly excited  $\text{Na}(n^2D)$  atom colliding with inert gas atoms. 1—experiment<sup>169, 170</sup>; theory: 2—Ref. 189, 3—Ref. 190; 4—Eq. (53).

is the quantum defect (see Tables I and II). The Massey parameter equals

$$\zeta \sim \frac{\Delta E_a}{v_a} \sim \frac{\delta_l}{nv_a}, \quad (55)$$

where the quantum defect is taken for the state with the smallest  $l$ . For  $l > 1$ , due to the smallness of the quantum defect, the Massey parameter turns out to be small and the corresponding transitions occur freely. A different situation arises in the case of a transition involving highly excited states with orbital angular momentum  $l=0, 1$ . In these cases, the Massey parameter satisfies  $\zeta \geq 1$  for values of  $n$  that are not too high. Then, the transition probability during collisions is determined by the particular form of the potential curves of the electron energy for neighboring states and the transitions occur near the regions where these curves approach each other. Accordingly, the cross section for the transition in this case is significantly less than the cross-sectional area of the excited atom.

We note that Eq. (50), as well as Eqs. (53) and (54), reflect two different limiting cases for quenching of the highly excited atomic states in the case that the interaction between the atom and the incident atomic particle is of short range. In the former case condition (49) is satisfied, according to which the uncertainty in energy over the collision time  $1/\tau$  is much less than the transition energy  $\Delta E$ . In this case, the transition itself involves many transitions near the points of intersection and of pseudointersection of the levels. In the latter case, the transition occurs between the states of interest with nearly equal energies. The relative shift in the phases of the wave functions for these states over the collision time is small, and this permits replacing expressions of the form  $\exp(i\Delta Et)$  with unity in formulas for the probability of transitions between these states.

Especially efficient quenching of highly excited atomic states occurs in collisions with molecules. This problem was studied theoretically<sup>193, 205</sup> as well as experimentally.<sup>206</sup> The process of interest proceeds according to the following scheme:



Using the expressions obtained, let us determine the cross section for the process (56) for collisions with dipole molecules in the case of low collision speeds  $v_a \ll 1/n$ . According to Eq. (39), we have for the cross section of the process (56):

$$\sigma_{\text{quench}} = \frac{\langle v\sigma_{el} \rangle}{v_a} \quad (57)$$

where  $\sigma_{el}$  is the cross section for elastic scattering of an electron by the molecule, which we can determine from perturbation theory<sup>207</sup>

$$\sigma_{el} = \frac{8\pi D^2}{3v_a^2},$$

where  $D$  is the dipole moment of the molecule. Substituting this formula into Eq. (57), we obtain

$$\sigma_{\text{quench}} = \frac{1}{v_a} \frac{8\pi}{3} D^2 \left\langle \frac{1}{v} \right\rangle = \frac{128D^2 n}{9v_a}. \quad (58)$$

Equation (58) is valid when condition (53a) is satisfied. The magnitude of the cross section (58) is significantly

greater than that computed according to Eqs. (45) and (46), where the cross section for an inelastic transition between rotational levels was used. The ratio of these cross sections coincides with the ratio of the left and right sides of (43a).

The quenching processes examined above for highly excited states involve a change in the population of the given levels. The experimental study of these processes is based on this fact. Other reactions involving collisions of highly excited atoms with neutral atomic particles involve a change in the phase characteristics of the states while their population remains constant. The experimental study of such relaxation processes for highly excited states is reduced to measuring the cross section corresponding to the broadening of spectral lines,<sup>208-212</sup> as well as the cross section for depolarization of the state by single-photon and two-photon transitions.<sup>213</sup> These cross sections are much greater than the quenching cross sections for excited states and are determined by interference effects during collisions. Since these processes depend on the nature of the interference phenomena under particular conditions, rather than on the nature of the interaction between the particles, these processes are not examined here.

## 8. CONCLUSIONS

Highly excited atomic states are very simple quantum systems that consist of a bound state of an electron and an atomic core interacting according to Coulomb law. For this reason, the theoretical study of such systems is based on quantum mechanics, which has provided an understanding of many of the properties of these systems as well as of the nature of the processes in which such systems participate. The experimental techniques developed in recent years, which permit producing and studying highly excited atoms in selected states, has provided new information concerning highly excited atoms. This has not only extended the range of scientific investigations, but has also opened up unexpected applications involving highly excited atoms. Not all such possibilities have been exploited, but there is no doubt that future studies of highly excited atoms will lead to the creation of fine and precise instrumentation with fundamentally new properties.

The author is grateful to S. E. Kupriyanov and L. P. Presnyakov for valuable remarks.

<sup>1</sup>A. K. Dupree and L. Goldberg, *Ann. Rev. Astron. and Astrophys.* **8**, 231 (1970).

<sup>2</sup>T. R. Carson and M. J. Roberts, *Atoms and Molecules in Astrophysics*, Academic Press, London, 1972.

<sup>3</sup>M. Brocklehurst and M. J. Seaton, *Mon. Not. Roy. Astron. Soc.* **157**, 179 (1972).

<sup>4</sup>E. J. Chaisson and M. A. Malkan, *Astrophys. J.* **210**, 108 (1976).

<sup>5</sup>K. Takayanagi, *Comm. Atom. Mol. Phys.* **6**, 177 (1977).

<sup>6</sup>V. Pankonin, P. Thomasson, and J. Barsuhn, *Astron. and Astrophys.* **54**, 335 (1977).

<sup>7</sup>W. B. Somerville, *Rept. Progr. Phys.* **40**, 483 (1977).

<sup>8</sup>D. R. Sweetman, *Nucl. Fusion, Suppl.* **1**, 279 (1962).

<sup>9</sup>A. C. Riviere and D. R. Sweetman, *Proc. Sixth Inter. Conf.*

- on Ionization Phenomena in Gases, Paris, 1963, p. 105.
- <sup>10</sup>N. F. Fedorenko, V. A. Ankudinov, and O. N. Il'in, Zh. Tekh. Fiz. **35**, 585 (1965) [Sov. Phys. Tech. Phys. **10**, 461 (1965)].
- <sup>11</sup>C. E. Moore, Atomic Energy Levels, National Bureau of Standards, Washington, Vol. I (1949); *ibid.*, Vol. II (1952); *ibid.*, Vol. III (1957).
- <sup>12</sup>P. Esherick, Phys. Rev. A **15**, 1920 (1977).
- <sup>13</sup>D. Kleppner and T. W. Ducas, Bull. Am. Phys. Soc. **21**, 600 (1976).
- <sup>14</sup>T. F. Gallagher *et al.*, Phys. Rev. A **15**, 1937 (1977).
- <sup>15</sup>T. W. Ducas and M. L. Zimmerman, *ibid.* **15**, 1523 (1977).
- <sup>16</sup>H. Bethe and E. Salpeter, Quantum Mechanics of One- and Two-Electron Atoms, Academic Press, N. Y., 1957. (Russ. Transl., IL, M. 1970).
- <sup>17</sup>L. D. Landau and E. M. Lifshitz, Kvantovaya Mekhanika, Fizmatgiz, Moscow, 1974 [Quantum Mechanics, Pergamon Press, N. Y. (1977)].
- <sup>18</sup>W. C. Martin, J. Res. Nat. Bur. Stand. A **64**, 79 (1960).
- <sup>19</sup>W. H. Wing, K. R. Lea, and W. E. Lamb in Atomic Physics Vol. III ed. by S. J. Smith and G. K. Walters, Plenum Publishing Co., New York, 1973, p. 119.
- <sup>20</sup>C. Fabre and S. Haroche, Opt. Commun. **13**, 393 (1975).
- <sup>21</sup>K. Fredriksson and S. Svanberg, J. Phys. B **9**, 1237 (1976).
- <sup>22</sup>R. N. Il'in *et al.*, Zh. Eksp. Teor. Fiz. **47**, 1235 (1964) [Sov. Phys. JETP **20**, 835 (1965)].
- <sup>23</sup>N. V. Fedorenko, V. A. Ankudinov, and R. N. Il'in, Zh. Tekh. Fiz. **35**, 585 (1965) [Sov. Phys. Tech. Phys. **10**, 461 (1965)].
- <sup>24</sup>R. N. Il'in *et al.*, Zh. Tekh. Fiz. **36**, 1241 (1966) [Sov. Phys. Tech. Phys. **11**, 921 (1967)].
- <sup>25</sup>V. A. Oparin, R. N. Il'in, and E. S. Solov'ev, Zh. Eksp. Teor. Fiz. **52**, 369 (1967) [Sov. Phys. JETP **25**, 240 (1967)].
- <sup>26</sup>J. R. Hiskes, Phys. Rev. **180**, 146 (1969).
- <sup>27</sup>R. LeDoucen and J. Guidini, C. R. Acad. Sci. Ser. B **268**, 918 (1969).
- <sup>28</sup>K. H. Berkner *et al.*, Phys. Rev. **182**, 103 (1969).
- <sup>29</sup>R. N. Il'in *et al.*, Zh. Eksp. Teor. Fiz. **59**, 103 (1969) [Sov. Phys. JETP **32**, 59 (1971)].
- <sup>30</sup>J. E. Bayfield and P. M. Koch, Phys. Rev. Lett. **33**, 258 (1974).
- <sup>31</sup>J. E. Bayfield, G. A. Khayrallah, and P. M. Koch, Phys. Rev. A **9**, 209 (1974).
- <sup>32</sup>P. M. Koch and J. E. Bayfield, Phys. Rev. Lett. **34**, 448 (1975).
- <sup>33</sup>J. E. Bayfield in The Physics of Electronic and Atomic Collisions, ed. by J. S. Risley and R. Geballe, University of Washington Press, Seattle, 1976, p. 726.
- <sup>34</sup>V. Cermak and Z. Herman, Coll. Czech. Comm **29**, 953 (1964).
- <sup>35</sup>S. E. Kupriyanov, Zh. Eksp. Teor. Fiz. **48**, 467 (1965) [Sov. Phys. JETP **21**, 311 (1965)]; *ibid.*, **51**, 1011 (1966) [Sov. Phys. JETP **24**, 674 (1967)]; *ibid.*, **55**, 460 (1968) [Sov. Phys. JETP **28**, 240 (1969)].
- <sup>36</sup>S. E. Kupriyanov, Opt. Spectrosc. **20**, 163 (1966) [Opt. Spectrosc. (USSR) **20**, 85 (1966)].
- <sup>37</sup>H. Hotop and A. Niehaus, J. Chem. Phys. **47**, 2506 (1967); Zs. Phys. Bd. **215**, S. 395 (1968).
- <sup>38</sup>T. Shibata, T. Kukuyama, and K. Kuchitsu, Bull. Chem. Soc. Japan, **47**, 2883 (1974).
- <sup>39</sup>J. A. Stockdale *et al.*, J. Chem. Phys. **60**, 4279 (1974).
- <sup>40</sup>C. E. Klots, *ibid.*, **66**, 5240 (1977).
- <sup>41</sup>J. A. Schiavone, Phys. Rev. A **16**, 48 (1977).
- <sup>42</sup>J. A. Schiavone, S. M. Tarr, and R. S. Freund, *ibid.*, **20**, 71 (1979).
- <sup>43</sup>I. L. Beigman, L. A. Vainshtein, and R. A. Syunyaev, Usp. Fiz. Nauk **95**, 267 (1968) [Sov. Phys. Usp. **11**, 411 (1968)].
- <sup>44</sup>W. L. Borst and E. C. Zipf, Phys. Rev. A **4**, 153 (1971).
- <sup>45</sup>R. S. Freund, J. Chem. Phys. **54**, 3125 (1975).
- <sup>46</sup>K. C. Smyth, J. A. Schiavone, and R. S. Freund, *ibid.*, **59**, 5225 (1973); *ibid.*, **60**, 1358 (1974).
- <sup>47</sup>J. A. Schiavone, K. C. Smyth, and R. S. Freund, *ibid.*, **63**, 1043 (1975).
- <sup>48</sup>T. G. Finn *et al.*, *ibid.*, **63**, 1596 (1975).
- <sup>49</sup>W. C. Wells, W. L. Borst, and E. C. Zipf, Phys. Rev. A **14**, 695 (1976).
- <sup>50</sup>S. E. Kupriyanov, Pis'ma Zh. Eksp. Teor. Fiz. **5**, 245 (1967) [JETP Lett. **5**, 197 (1967)].
- <sup>51</sup>J. F. Delpech, J. Boulmer, and F. Devos, Phys. Rev. Lett. **39**, 1400 (1977).
- <sup>52</sup>F. Devos, J. Boulmer, and J. F. Delpech, J. de Phys. **40**, 215 (1979).
- <sup>53</sup>G. Baran *et al.*, in Proc. 11th Inter. Conf. on Physics of Electron and Atomic Collisions, Kyoto, 1979, p. 952.
- <sup>54</sup>S. Liberman and J. Pinard, Phys. Rev. A **20**, 507 (1979).
- <sup>55</sup>H. T. Duong, S. Liberman, J. Pinard, Opt. Commun. **18**, 533 (1976).
- <sup>56</sup>D. Popescu *et al.*, Phys. Rev. A **9**, 1182 (1974).
- <sup>57</sup>P. Esherick *et al.*, Phys. Rev. Lett. **36**, 1296 (1976).
- <sup>58</sup>Y. Kato and B. P. Stoicheff, J. Opt. Soc. Am. Lett. **66**, 490 (1976).
- <sup>59</sup>K. C. Harvey and B. P. Stoicheff, Phys. Rev. Lett. **38**, 537 (1977).
- <sup>60</sup>P. M. Koch, *ibid.*, **41**, 99 (1978).
- <sup>61</sup>P. M. Koch, J. B. Bowlin, and B. Mariana, cited in Ref. 53, p. 956.
- <sup>62</sup>I. I. Sobel'man, Vvedenie v teoriyu atomnykh spektrov, Fizmatgiz, Moscow, 1963 (Introduction to the Theory of Atomic Spectra, Pergamon Press, New York, 1972).
- <sup>63</sup>H. A. Kramers, Phil. Mag. **46**, 836 (1923).
- <sup>64</sup>W. Gordon, Ann. Phys. **2**, 1031 (1929).
- <sup>65</sup>P. F. Naccache, J. Phys. Ser. B **5**, 1308 (1972).
- <sup>66</sup>I. C. Percival and D. Richards, Adv. At. Mol. Phys. **11**, 2 (1975).
- <sup>67</sup>S. E. Kupriyanov in Fizika elektronnykh i atomnykh stolknovenii: lektzii 4 Vsesoyuznoi shkoly po fizike elektronnykh i atomnykh stolknovenii (Physics of Electronic and Atomic Collisions: Lectures at the 4th All-Union School on Physics of Electronic and Atomic Collisions), Izdatel'stvo Moskovskogo universiteta, Moscow, 1978, p. 43.
- <sup>68</sup>G. A. Surskii and S. E. Kupriyanov, Zh. Eksp. Teor. Fiz. **54**, 109 (1968) [Sov. Phys. JETP **27**, 61 (1968)].
- <sup>69</sup>P. Camus and C. Morillon, J. Phys. B **10**, L133 (1977).
- <sup>70</sup>A. V. Chaplik, Zh. Eksp. Teor. Fiz. **54**, 332 (1968) [Sov. Phys. JETP **27**, 178 (1968)].
- <sup>71</sup>H. R. Trautenberg, R. Gebauer, and G. Lewin, Naturwissenschaften Bd. **18**, S. 417 (1930).
- <sup>72</sup>C. Lanczos, Zs. Phys. **62**, 518 (1930); **68**, 204 (1931).
- <sup>73</sup>H. Bethe, Quantum Mechanics of the Simplest Systems [Russ. Transl., ONTI, Moscow, Leningrad, 1935, p. 193].
- <sup>74</sup>A. C. Riviere in Methods of Experimental Physics, Vol. 7A, ed. by B. Bederson and W. L. Fite, Academic Press, New York, 1968, p. 208.
- <sup>75</sup>B. M. Smirnov, Atomnye stolknoveniya i elementarnye protsessy v plazme (Atomic Collisions and Elementary Processes in Gases), Atomizdat, Moscow, 1968.
- <sup>76</sup>V. S. Letokhov, V. I. Mitin, and A. A. Pureskii in Khimiya plazmy (The Chemistry of Plasma), Atomizdat, Moscow, 1977, No. 4, p. 3.
- <sup>77</sup>J. E. Bayfield, Phys. Rept. **6**, 317 (1979).
- <sup>78</sup>M. H. Rice and R. H. Good, J. Opt. Soc. Am. **52**, 239 (1962).
- <sup>79</sup>B. M. Smirnov and M. I. Chibisov, Zh. Eksp. Teor. Fiz. **49**, 841 (1965) [Sov. Phys. JETP **22**, 585 (1966)].
- <sup>80</sup>T. W. Ducas *et al.*, Phys. Rev. Lett. **35**, 366 (1975).
- <sup>81</sup>R. G. Stebbings *et al.*, Phys. Rev. A **12**, 1453 (1975).
- <sup>82</sup>T. F. Gallagher *et al.*, *ibid.*, **16**, 1098 (1977).
- <sup>83</sup>D. R. Bates and G. Griffing, Proc. Phys. Soc. **66**, 961 (1953).
- <sup>84</sup>M. J. Seaton, *ibid.*, **79**, 1105 (1962).
- <sup>85</sup>G. C. McCoyd and S. N. Milford, Phys. Rev. **130**, 206 (1963).
- <sup>86</sup>H. E. Saraph, Proc. Phys. Soc. **83**, 763 (1964).
- <sup>87</sup>L. A. Vainshtein, Opt. Spektrosk. **18**, 538 (1965) [Opt. Spectrosc. (USSR) **18**, 538 (1965)].
- <sup>88</sup>K. Omidvar, Phys. Rev. A **140**, 38 (1965).
- <sup>89</sup>A. D. Stanffer and M. R. C. McDowell, Proc. Phys. Soc. **85**,

- 61 (1965); *ibid.*, 89, 289 (1966).
- <sup>90</sup>A. E. Kingston and J. E. Lauer, *ibid.*, 87, 399 (1966); *ibid.* 88, 597 (1966).
- <sup>91</sup>D. S. Crothers and A. R. Holt, *ibid.*, 88, 75 (1966).
- <sup>92</sup>A. N. Starostin, Zh. Eksp. Teor. Fiz. 52, 124 (1967) [Sov. Phys. JETP 25, 80 (1967)].
- <sup>93</sup>L. I. Podlubnyĭ, Opt. Spektrosk. 22, 359 (1967) [Opt. Spectrosc. (USSR) 22, 359 (1967)].
- <sup>94</sup>L. I. Podlubnyĭ and V. M. Sergeev, *ibid.*, 27, 216 (1969), *ibid.* 27, 216 (1969)].
- <sup>95</sup>I. L. Beigman, A. M. Urnov, and V. P. Shevel'ko, Zh. Eksp. Teor. Fiz. 31, 978 (1970) [Sov. Phys. JETP 31, 978 (1970)].
- <sup>96</sup>L. C. Johnson, Astrophys. J. 174, 227 (1972).
- <sup>97</sup>M. Gryzinski, Phys. Rev. 115, 374 (1959); *ibid.*, 138A, 305 (1965).
- <sup>98</sup>R. Abrines, I. C. Percival, and N. A. Valentine, Proc. Phys. Soc. 89, 515 (1966).
- <sup>99</sup>V. D. Brattsev and V. I. Ochkur, Zh. Eksp. Teor. Fiz. 52, 955 (1967) [Sov. Phys. JETP 25, 631 (1967)].
- <sup>100</sup>A. Burgess and I. C. Percival, Adv. At. Mol. Phys. 4, 109 (1968).
- <sup>101</sup>P. Mansbach and J. C. Keck, Phys. Rev. 181, 275 (1969).
- <sup>102</sup>I. C. Percival and D. Richards, J. Phys. B 3, 1035 (1970).
- <sup>103</sup>J. C. Keck, Adv. At. Mol. Phys. 8, 39 (1972).
- <sup>104</sup>D. R. Bates and R. Snyder, J. Phys. B 6, 642 (1973).
- <sup>105</sup>M. Gryzinski, J. Kunk, and Q. Zgorzelskiĭ, *ibid.*, 6, 2292 (1973).
- <sup>106</sup>I. C. Percival and D. Richards, Adv. At. Mol. Phys. 11, 2 (1975).
- <sup>107</sup>J. F. Delpach, J. Boulmer, and J. Stevefelt, Adv. Electron. Electron Phys. 39, 121 (1975).
- <sup>108</sup>I. L. Beigman, L. A. Vainshtein, and I. I. Sobel'man, Zh. Eksp. Teor. Fiz. 57, 1703 (1969) [Sov. Phys. JETP 30, 920 (1970)].
- <sup>109</sup>L. P. Presnjakov and A. M. Urnov, J. Phys. B 5, 153 (1970).
- <sup>110</sup>I. L. Beigman, L. P. Presnjakov, and A. M. Uranov, P. N. Lebedev Physics Institute, Academy of Sciences of the USSR, Preprint No. 3, Moscow, 1975.
- <sup>111</sup>J. Thompson, Phil. Mag. 23, 449 (1912).
- <sup>112</sup>L. Thomas, Proc. Cambridge Phil. Soc. 28, 713 (1927).
- <sup>113</sup>D. Webster, W. Hansen, and F. Duveneck, Phys. Rev. 43, 883 (1933).
- <sup>114</sup>H. Bethe, Ann. Phys. 4, 325 (1930).
- <sup>115</sup>A. E. Kingston, Phys. Rev. A 135, 1537 (1964).
- <sup>116</sup>A. E. Kingston, Proc. Phys. Soc. 87, 193 (1966).
- <sup>117</sup>J. D. Garcia, Phys. Rev. 177, 223 (1967).
- <sup>118</sup>A. E. Kingston, J. Phys. B 1, 559 (1968).
- <sup>119</sup>L. A. Sena, Zh. Eksp. Teor. Fiz. 9, 1320 (1939).
- <sup>120</sup>L. A. Sena, Stolknoveniya elektronov i ionov s atomami gaza (Collisions of Electrons and Ions with Gas Atoms), Gostekhizdat, Moscow, 1948.
- <sup>121</sup>L. A. Vainshtein, I. I. Sobel'man, and E. A. Yukov, Vozbuzhdenie atomov i ushirenie spektral'nykh liniĭ (Excitation of Atoms and Broadening of Spectral Lines), Nauka, Moscow, 1975, Section 10.
- <sup>122</sup>I. V. Komarov, L. I. Ponomarev, and S. Yu. Slavyanov, Sferoidal'nye i kulonovskie sferoidal'nye funktsii (Spheroidal and Coulomb Spheroidal Functions), Nauka, Moscow, 1976.
- <sup>123</sup>D. R. Bates and R. A. Mapleton, Proc. Phys. Soc. 87, 657 (1966).
- <sup>124</sup>D. R. Bates and R. H. G. Reid, J. Phys. B 2, 851 (1969).
- <sup>125</sup>D. R. Bates and R. H. G. Reid, *ibid.*, 2, 887 (1969).
- <sup>126</sup>B. M. Smirnov, Zh. Eksp. Teor. Fiz. 59, 1226 (1970) [Sov. Phys. JETP 32, 670 (1971)].
- <sup>127</sup>B. M. Smirnov, Asimptoticheskie metody v teorii atomnykh stolknoveniiĭ (Asymptotic methods in the Theory of Atomic Collisions), Atomizdat, Moscow, 1973.
- <sup>128</sup>N. Toshima, J. Phys. Soc. Japan 46, 927 (1979)1; *ibid.*, 46, 1295 (1979); *ibid.* 47, 257 (1979).
- <sup>129</sup>N. Toshima, cited in Ref. 53, p. 958.
- <sup>130</sup>E. E. Nikitin and B. M. Smirnov, Usp. Fiz. Nauk 124, 201 (1978) [Sov. Phys. Usp. 21, 95 (1978)].
- <sup>131</sup>B. M. Smirnov, Fizika slabionizovannogo gaza (Physics of a Weakly Ionized Gas), Nauka, Moscow, 1972, p. 131.
- <sup>132</sup>B. M. Smirnov, Iony i vozbuzhdennye atomy v plazme (Ions and Excited Atoms in Plasma), Atomizdat, Moscow, 1974.
- <sup>133</sup>B. M. Smirnov, cited in Ref. 33, p. 701.
- <sup>134</sup>S. T. Butler and R. M. May, Phys. Rev. A 137, 10 (1965).
- <sup>135</sup>P. M. Koch, Phys. Rev. Lett. 43, 432 (1979).
- <sup>136</sup>P. M. Koch, cited in Ref. 53, p. 956.
- <sup>137</sup>D. Mathur and J. B. Hasted, J. Phys. B 10, L265 (1977).
- <sup>138</sup>D. E. Golden, Adv. At. Mol. Phys. 14, 1 (1978).
- <sup>139</sup>M. Matsuzawa, J. Phys. Soc. Japan 32, 1088 (1972); *ibid.*, 33, 1108 (1972).
- <sup>140</sup>W. P. West *et al.*, Phys. Rev. Lett. 36, 1352 (1977).
- <sup>141</sup>G. W. Foltz *et al.*, J. Chem. Phys. 67, 1352 (1977).
- <sup>142</sup>G. F. Hildenbrandt *et al.*, J. Chem. Phys. 68, 1349 (1978).
- <sup>143</sup>A. A. Christodoulides and L. G. Christophorou, *ibid.*, 54, 4691 (1971).
- <sup>144</sup>F. J. Davis, R. N. Compton, and D. R. Nelson, *ibid.*, 59, 2324 (1973).
- <sup>145</sup>J. M. Warman and M. C. Sauer, *ibid.*, 52, 6428 (1970).
- <sup>146</sup>M. Matsuzawa, *ibid.* 55, 2685 (1971).
- <sup>147</sup>M. Matsuzawa, *ibid.* 58, 2679 (1973).
- <sup>148</sup>M. Matsuzawa, J. Electron. Spectrosc. 4, 1 (1974).
- <sup>149</sup>G. N. Fowler and T. W. Preist, J. Chem. Phys. 56, 1601 (1972).
- <sup>150</sup>T. W. Preist, J. Chem. Soc. Farad. Trans. pt. I 68, 661 (1972).
- <sup>151</sup>C. J. Latimer, J. Phys. B 10, 1889 (1977).
- <sup>152</sup>M. Matsuzawa, Preprint No. 3573, Tokyo University, 1979.
- <sup>153</sup>O. H. Crawford, A. Dalgarno, and P. B. Hays, Mol. Phys. 13, 181 (1967).
- <sup>154</sup>Y. Itikawa, J. Phys. Soc. Japan 30, 835 (1971).
- <sup>155</sup>E. Gerjuoy and S. Stein, Phys. Rev. 97, 1671 (1955).
- <sup>156</sup>H. Hotop and A. Niehaus, J. Chem. Phys. 47, 2506 (1967).
- <sup>157</sup>S. E. Kupriyanov, Zh. Eksp. Teor. Fiz. 51, 1011 (1966) [Sov. Phys. JETP 24, 674 (1967)].
- <sup>158</sup>H. Hotop and A. Niehaus, Zs. Phys. Bd. 215, S. 395 (1968).
- <sup>159</sup>S. E. Kupriyanov, Zh. Eksp. Teor. Fiz. 55, 460 (1968) [Sov. Phys. JETP 28, 240 (1969)].
- <sup>160</sup>G. W. Foltz *et al.*, in Proc. 5th Int. Conf. on Atomic Physics, 1976, p. 256.
- <sup>161</sup>M. Matsuzawa and W. A. Chupka, Chem. Phys. Lett. 50, 373 (1977).
- <sup>162</sup>R. F. Stebbings *et al.*, in Proc. 10th Int. Conf. on the Physics of Electronic and Atomic Collisions, Paris, 1977, p. 170.
- <sup>163</sup>K. A. Smith *et al.*, Phys. Rev. Lett. 40, 1362 (1978).
- <sup>164</sup>F. G. Keller, cited in Ref. 53, p. 948.
- <sup>165</sup>H. Hiraishi *et al.*, *ibid.*, p. 948.
- <sup>166</sup>T. Kondow *et al.*, *ibid.*, p. 950.
- <sup>167</sup>E. J. Beiting *et al.*, J. Chem. Phys. 70, 3551 (1979).
- <sup>168</sup>T. G. Gallagher and W. E. Cooke, Phys. Rev. Lett. 42, 835 (1979).
- <sup>169</sup>T. F. Gallagher, S. A. Edelstein, and R. M. Hill, *ibid.* 75, 644 (1975).
- <sup>170</sup>T. F. Gallagher, S. A. Edelstein, and R. M. Hill, Phys. Rev. A 15, 1945 (1977).
- <sup>171</sup>T. F. Gallagher, W. E. Cooke, and S. A. Edelstein, *ibid.* 17, 904 (1978).
- <sup>172</sup>T. F. Gallagher and W. E. Cooke, Bull. Am. Phys. Soc. 23, 1102 (1978).
- <sup>173</sup>T. F. Gallagher and W. E. Cooke, Phys. Rev. A 19, 2162 (1979).
- <sup>174</sup>A. Hitachi *et al.*, cited in Ref. 53, p. 944.
- <sup>175</sup>F. Gounand, P. R. Fournier, and J. Bertande, Phys. Rev. A 15, 1762212 (1977).
- <sup>176</sup>F. Gounand, P. R. Fournier, and M. Hugon, cited in Ref. 53, p. 930.
- <sup>177</sup>M. Hugon, P. R. Fournier, and F. Gounand, *ibid.*, p. 932.
- <sup>178</sup>M. Hugon *et al.*, *ibid.*, p. 934.
- <sup>179</sup>J. S. Deech *et al.*, J. Phys. B 10, L137 (1977).

- <sup>180</sup>L. R. Pendrill, *ibid.*, p. L469.
- <sup>181</sup>R. F. Stebbings, *Science* **193**, 537 (1976).
- <sup>182</sup>N. Mott and H. Massey, *Teoriya atomnykh stolknovenii*, Mir, Moscow, 1969 (*Theory of Atomic Collisions*, Clarendon Press, Oxford, 1965).
- <sup>183</sup>L. P. Pitaevskii, *Zh. Eksp. Teor. Fiz.* **42**, 1326 (1962) [*Sov. Phys. JETP* **15**, 919 (1962)].
- <sup>184</sup>D. R. Bates and S. P. Khare, *Proc. Phys. Soc.* **85**, 231 (1965).
- <sup>185</sup>M. R. Flannery, *Ann. Phys.* **61**, 465 (1970).
- <sup>186</sup>M. R. Flannery, *ibid.* **79**, 480 (1973).
- <sup>187</sup>M. Matsuzawa, *J. Chem. Phys.* **55**, 2685 (1971).
- <sup>188</sup>M. Matsuzawa, *ibid.* **58**, 2674 (1973).
- <sup>189</sup>M. Matsuzawa, *Phys. Rev. A* **9**, 241 (1974).
- <sup>190</sup>M. Matsuzawa, *J. Phys. B* **8**, 2114 (1975).
- <sup>191</sup>M. Matsuzawa, *ibid.* **9**, 2559 (1976).
- <sup>192</sup>M. Matsuzawa, *ibid.* **10**, 1543 (1977).
- <sup>193</sup>M. Matsuzawa, *Phys. Rev. A* **18**, 1396 (1978).
- <sup>194</sup>M. Matsuzawa, *ibid.* **19**, (1979).
- <sup>195</sup>M. Matsuzawa, *J. Phys. B* **1**, 3743 (1979).
- <sup>196</sup>N. L. Aleksandrov, *Zh. Eksp. Teor. Fiz.* **76**, 1236 (1979) [*Sov. Phys. JETP* **49**, 627 (1979)].
- <sup>197</sup>J. I. Gerstein, *Phys. Rev. A* **14**, 1354 (1976).
- <sup>198</sup>R. E. Olson, *ibid.* **15**, 631 (1977).
- <sup>199</sup>A. Omont, *J. de Phys.* **38**, 1343 (1977).
- <sup>200</sup>A. P. Hickman, *Phys. Rev. A* **18**, 1339 (1978).
- <sup>201</sup>J. Deronard and M. Lombardi, *J. Phys. B* **11**, 3875 (1978).
- <sup>202</sup>A. P. Hickman, *Phys. Rev. A* **19**, 994 (1979).
- <sup>203</sup>M. Matsuzawa, cited in Ref. 53, p. 942.
- <sup>204</sup>E. De Prunele and J. Pascale, *ibid.*, p. 928.
- <sup>205</sup>R. D. Rundol, *ibid.*, p. 936.
- <sup>206</sup>F. G. Kellert, *ibid.*, p. 948.
- <sup>207</sup>S. Altshuler, *Phys. Rev.* **107**, 114 (1957).
- <sup>208</sup>M. A. Mazing and N. A. Vrublevskaya, *Zh. Eksp. Teor. Fiz.* **50**, 343 (1965) [*Sov. Phys. JETP* **23**, 228 (1966)]; M. A. Mazing and P. D. Serapinas, *Zh. Eksp. Teor. Fiz.* **60**, 541 (1971) [*Sov. Phys. JETP* **33**, 294 (1971)].
- <sup>209</sup>A. Flusberg, T. W. Mossberg, and S. R. Haetmann, *Opt. Commun.* **24**, 207 (1978).
- <sup>210</sup>T. F. Gallagher and W. E. Cooke, *Phys. Rev. A* **19**, 820 (1979).
- <sup>211</sup>A. Flusberg *et al.*, *ibid.* **19**, 1607 (1979).
- <sup>212</sup>R. Kachru, T. W. Mossberg, and S. R. Haetmann, cited in Ref. 53, p. 948.
- <sup>213</sup>L. R. Pendrill and G. W. Series, *J. Phys. B* **11**, 4049 (1978).

Translated by M. E. Alferieff